A STUDY OF HIGH TEMPERATURE REACTIONS IN OXIDE-DISPERSION-STRENGTHENED MOLYBDENUM AT REDUCED OXYGEN PARTIAL PRESSURES

A Thesis
Presented to
The Academic Faculty

By

Jelila Sarah Mohammed

In Partial Fulfillment
Of the Requirements for the Degree
Master of Science in Materials Science and Engineering

Georgia Institute of Technology

July, 2004

A Study of High Temperature Reactions in
Oxide-Dispersion-Strengthened Molybdenum
at Reduced Oxygen Partial Pressures

Approved By:

Dr. David N. Hill

Dr. Janet M. Hampikian

Dr. Robert F. Speyer

Dr. Wayne L. Ohlinger

Date Approved July 8, 2004

ACKNOWLEDGEMENTS

There are several people who deserve my deepest gratitude, because without them this work would not have been possible. First of all, I would like to thank Dr. Norm Hill for his guidance, knowledge, and for giving me the opportunity to work on this project. Also, the members of my thesis committee, Dr. Wayne Ohlinger, Dr. Janet Hampikian, and Dr. Robert Speyer were a great help by giving their time to read my thesis and provide valuable suggestions and insight. The success of this research depended heavily on Richard Shafer's skill and expertise as he spent countless hours keeping the furnace and other equipment running smoothly, in spite of all of the challenges we faced.

I greatly appreciate the friendship of the other graduate students in the MSE department, including Kasi, Chuck, Kip, Dawn, Matt, Morgan, Chris, Will, Brent, Dan M., Rob, Shubhra, Dan C., Mike, Shawn, Larry, and Melissa. They have all made these past couple of years enjoyable and memorable. In particular, I would like to thank Laura for always being so understanding and supportive. Thanks are also due to Erin for her motivating, cheerful attitude (and for her jelly beans).

I am also especially grateful to Jeremy for having so much faith in me and for always being there for me. His unlimited patience, kindness, and encouragement kept me going during some of the most stressful and difficult times.

Finally, I thank my family for their love and support throughout my education. My parents have taught me some of life's most important lessons, and they have worked hard to provide me with so many great opportunities in and outside of school. Also, my sister, Naila, has been very thoughtful, caring, and encouraging over the years. My

family has always believed in my abilities, sometimes even more than I did, and my accomplishments would not have been possible without their motivation and encouragement.

TABLE OF CONTENTS

ACKNOWLEDGEMENTS iii

LIST OF TABLES vii

LIST OF FIGURES viii

SUMMARY x

CHAPTER 1 INTRODUCTION 1

CHAPTER 2 LITERATURE REVIEW 3
- Ferroelectrics 3
- Dispersion Strengthening 4
- Rare Earth Molybdates 5
- Phase Equilibria Studies 6
- Preparation Techniques 8
- The La_2O_3-MoO_3 System 10
- The La_2O_3-MoO_2 System 12
- The La_2O_3-MoO_2-MoO_3 System 12
- The Y_2O_3-MoO_x System 13
- The ZrO_2-MoO_x System 17
- The CeO_2-MoO_x System 18

CHAPTER 3 EXPERIMENTAL PROCEDURE 20
- Preparation and Processing of Samples 20
- Experimental Setup 21
- Temperature Control 24
- Atmosphere Control 25
- Characterization 27

CHAPTER 4 RESULTS AND DISCUSSION 28
- $LaO_{1.5}$-MoO_x system at 1200°C 29
  - Oxygen Partial Pressures from $1x10^{-4}$ to $2x10^{-6}$ Pa 32
  - Oxygen Partial Pressures from 2x10-6 to 3x10-7 Pa 32
  - Oxygen Partial Pressure of 3x10-7 to 1x10-7 Pa 37
  - Oxygen Partial Pressure of 1x10-7 to 8x10-9 Pa 42
  - Oxygen Partial Pressure below 8x10-9 Pa 52
- The $LaO_{1.5}$-MoO_x system at 1000ºC 55
- The $YO_{1.5}$-MoO_x system at 1200ºC 58
- The $YO_{1.5}$-MoO_x system at 1000ºC 61
- The ZrO_2-MoO_x system 62

CHAPTER 5 CONCLUSIONS 64

CHAPTER 6 RECOMMENDATIONS 66

APPENDICES 68

REFERENCES 71

LIST OF TABLES

Table 3.1 Heating and cooling rates for furnace 25

Table 4.1 Phases resulting from experiments with La_2O_3 and Mo at 1200°C 30

Table 4.2 Phases resulting from experiments with La_2O_3 and Mo at 1000°C 57

Table 4.3 Phases resulting from experiments with Y_2O_3 and Mo at 1200°C 58

Table 4.4 Phases resulting from experiments with Y_2O_3 and Mo at 1000°C 61

Table 4.5 Phases resulting from experiments with ZrO_2 and Mo 63

LIST OF FIGURES

Figure 2.1 MoO_3-La_2O_3 Phase Diagram 11

Figure 2.2 MoO_3-Y_2O_3 Phase Diagram 15

Figure 3.1 Process Flow Diagram 21

Figure 3.2 Tube Furnace Used for Heating Samples 22

Figure 3.3 End Plate at Inlet of Furnace Tube with Pressure Gauge 23

Figure 3.4 End Plate at the Outlet of the Furnace Tube 23

Figure 3.6 Partial pressure of O_2 vs. fraction of CO_2 in the gas flow 26

Figure 4.1 Phase equilibria in the $LaO_{1.5}$-MoO_x system at 1200ºC 31

Figure 4.2 XRD Pattern for LAMO_53 34

Figure 4.3 XRD pattern for LAMO_10 35

Figure 4.4 XRD Pattern for LAMO_54 36

Figure 4.5 XRD Pattern for LAMO_60 39

Figure 4.6 XRD Pattern for LAMO_61 40

Figure 4.7 XRD Pattern for LAMO_62 41

Figure 4.8 XRD Pattern for LAMO_35 43

Figure 4.9 XRD Pattern for LAMO_34 46

Figure 4.10 XRD Pattern for LAMO_34 with Powder Diffraction File for $Y_5Mo_2O_{12}$ 47

Figure 4.11 XRD Pattern for LAMO_66 50

Figure 4.12 XRD Pattern for LAMO_31B 51

Figure 4.13 XRD Pattern for LAMO_20 53

Figure 4.14 XRD Pattern for LAMO_30 54

Figure 4.15 Phase equilibria in the $LaO_{1.5}$-MoO_x system at 1000ºC 56

Figure 4.16 XRD Pattern for Sample YMO_03 60

SUMMARY

Metal-oxide alloys containing Mo with a rare-earth oxide are of interest for high-temperature structural applications. It is unknown what specific compounds, phases, and crystal structures provide the properties of these high strength, deformable metal-oxides. This project intends to define phase equilibria of systems containing molybdenum and a rare-earth oxide, specifically La_2O_3, Y_2O_3, and ZrO_2 at high temperatures and low oxygen partial pressures.

Preceding research defined rare-earth molybdate phases of 2:1 La:Mo compositions at 1200°C at oxygen partial pressures ranging from 10^{-10} Pa to 10^{-7} Pa. This study aimed to identify phase boundaries in the La_2O_3-Mo, Y_2O_3-Mo, and ZrO_2-Mo systems at 1000°C and 1200°C at similar partial pressures of oxygen. Experiments in the La system were extended to focus on phases at several different La:Mo molar ratios.

Preliminary experiments in the Y_2O_3-Mo and ZrO_2-Mo systems were designed to investigate the formation of rare-earth molybdates with various oxidation levels of Mo. Phases and compounds were produced using powder starting materials reacted in a tube furnace under controlled oxygen partial pressures. Characterization was performed using x-ray diffraction, using published powder diffraction files for phase identification.

Regions of stability and specific processing conditions were identified for mixed-molybdenum valence phases in the La_2O_3-MoO_x system at 1200ºC ($La_{12}Mo_6O_{35}$, $La_4Mo_2O_{11}$, and $La_6Mo_2O_{14}$). A compound was formed at a 1:1.5 molar ratio of La:Mo between O_2 partial pressures of $3x10^{-7}$ Pa and $8x10^{-9}$ Pa for which the formula $La_2Mo_3O_{10}$ (with 2 Mo^{IV} for 1 Mo^{VI}) is suggested.

For samples run at a 2:1 La:Mo molar ratio, XRD patterns reveal the existence of a La-rich phase in equilibrium with Mo or a Mo-rich phase. Based on previously reported compounds of the form $Ln_5Mo_2O_{12}$ with a mixed molybdenum valence of 3 Mo^{IV} and 1 Mo^{VI}, this compound is believed to be $La_{10}Mo_4O_{24}$.

Experiments in the LaO_3-Mo system at 1000ºC confirmed previous work, but generated no new information due to the stability of Mo_2C versus rare-earth molybdates at low O_2 partial pressures obtained in CO_2-H_2 atmospheres.

XRD patterns from experiments with Y_2O_3 revealed the existence of a mixed-molybdenum valence phase, $Y_5Mo_2O_{12}$, at both 1200ºC and 1000ºC. Preliminary experiments in the ZrO_2-Mo system did not yield any rare-earth molybdates.

This study has defined much of the phase equilibria in the La_2O_3-Mo systems, as well as specific processing conditions for some of the molybdates formed at high temperatures at very low oxygen partial pressures. Further work should concentrate on producing samples of these pure phases suitable for mechanical testing, to help define the variables that contribute to the unique mechanical properties of rare-earth molybdates. Additional research is also necessary in the Y_2O_3-Mo and ZrO_2-Mo systems, particularly in the area of mixed-molybdenum valence compounds, which may help elucidate the effect of crystallography on plastic deformability in these compounds.

CHAPTER 1

INTRODUCTION

For years, rare-earth molybdates have been known for their ferro-electric properties, but more recently they have been hypothesized to form in oxide dispersion strengthened molybdenum (ODS-Mo) alloys. These alloys are produced by dispersing particles of certain rare-earth oxides (REO) in a molybdenum matrix and forming the mixture into a composite ingot. During the high-temperature consolidation process, the oxides may be converted into rare-earth molybdates. During subsequent processing, the oxide molybdate phase(s) undergo(es) deformation to form high-surface-area ribbons that serve to inhibit dislocation movement, thus improving the mechanical properties relative to pure molybdenum or solution-strengthered alloys, such as Mo-Re. Rare-earth oxides used in oxide dispersion strengthening are observed to provide excellent strength and display deformability. It has been suggested that this may be due to the presence of molybdate compounds rather than pure dispersed rare-earth oxide particles. The mechanical properties of oxide dispersion strengthened molybdenum are somewhat variable, and the formation of various rare-earth molybdates based on variations in processing details may explain, at least in part, why it is difficult to achieve highly reproducible behavior in processed alloys. It is also considered likely that molybdenum may display a range of oxidation states (IV to VI) in these rare-earth molybdates.

It is unknown what specific compounds and associated crystal structures may provide these oxides with their high strength and deformability. Likewise, little is known of the phase equilibria in rare-earth oxide- (metallic) molybdenum systems due to the high temperatures and low oxygen partial pressures required to evaluate them. The

primary goal of this research was to study phase equilibria in systems comprised of metallic molybdenum in equilibrium with rare-earth oxides or molybdate compounds. The project had the objective of identifying compounds and specific oxidation states of molybdenum over a range of equilibrium conditions. At temperatures of 1000ºC and 1200ºC, and O_2 partial pressures ranging from 10^{-4} Pa to 10^{-13} Pa, the systems $LaO_{1.5}$-Mo, $YO_{1.5}$-Mo, and ZrO_2-Mo were investigated.

A survey of the literature is given in Chapter 2, covering background information on the properties of rare-earth molybdates and related work on phase equilibria in these systems. The experimental procedure is explained in detail in Chapter 3. Using powder starting materials, samples of varying REO-Mo molar ratios were mixed and heated in a tube furnace with a controlled atmosphere. Various oxygen partial pressures were used to equilibrate compounds displaying Mo^{IV}, Mo^{VI}, and mixed-valence states. The oxygen partial pressure in the system was controlled using a mixed flow of H_2 and CO_2 gas. X-ray diffraction was used to identify phases in the samples. Chapter 4 presents the results of the experiments, with discussion of their significance. After identifying equilibrium phase compositions and molybdenum oxidation states as a function of oxygen partial pressure and temperature, phase diagrams were produced for the $LaO_{1.5}$-Mo system at 1200ºC and 1000ºC. These are binary phase diagrams that represent the data by means of oxygen partial pressure versus molar composition of MoO_x. Also, tentative formulas have been given for new phases that were identified using x-ray diffraction. The conclusions are summarized in Chapter 5. Finally, suggestions for future work are provided in Chapter 6.

CHAPTER 2

LITERATURE REVIEW

This chapter will serve as a broad survey of the literature on rare-earth molybdates. A brief discussion of the applications of rare-earth molybdates will be presented first, followed by a detailed account of research done on the phase equilibria of these systems. Many phases and compounds that possess varying and mixed Mo valences will be discussed in relation to the phase equilibria and published phase diagrams. The advancements in preparation and experimental techniques for these materials will also be addressed. The greater part of this review will focus on the lanthanum molybdates formed in both binary and ternary systems. Phase equilibria of the Y_2O_3-MoO_x system will also be presented for comparison to the La_2O_3-MoO_x system. Finally, literature on the related system, ZrO_2-MoO_x, will be examined.

Ferroelectrics

Great interest in the physical and structural properties of rare-earth molybdates was triggered in the 1960's in the field of ferroelectrics. In 1966, Borchardt and Bierstedt prepared a new material, $Gd_2(MoO_4)_3$, and found that it could be used as a ferroelectric laser host.[1] After this discovery, much research was aimed toward the synthesis and characterization of new compounds incorporating other rare-earth oxides and molybdenum. Most of the early studies focused on compounds containing $Mo^{VI}O_3$ instead of the reduced formulas that incorporate $Mo^{IV}O_2$. As research progressed into the late 1970's, discoveries were made of rare-earth molybdates containing mixed molybdenum valences. Structural and crystallographic data were characterized for these

materials, and the methods of preparation were refined to include solid-state reaction, fused salt electrolysis, and precipitation.

Dispersion Strengthening

Oxide dispersion strengthening has been used for years as a strengthening mechanism for metals. An oxide phase is mixed into a base metal by a variety of methods including mixing, sol/gel processing, and mechanical alloying. The deformability of the dispersoid particles is dependent on the following factors: oxide properties, particle size, deformation resistance of the base metal, and the interaction between the metal and oxide.[2] Most oxide particles behaved as expected with molybdenum, either with no change or breakage during deformation. Rare earth oxides, however, have been found to plastically deform. In 1990, Endo, *et al.*, experimentally doped molybdenum wire with five different rare earth oxides (Y_2O_3, La_2O_3, Nd_2O_3, Sm_2O_3, and Gd_2O_3). They found that doping increased the recrystallization temperature and reduced deformation at high temperatures when compared to undoped wire.[3] A 1992 study focused on the deformation of La_2O_3 particles in a Mo matrix due to the high particle deformability of La_2O_3 as opposed to other rare-earth oxides. The samples were rolled into sheets and drawn into wire to deform the oxides. Particle deformability was found to be closely related to the extent of rare-earth oxide dispersion strengthening in molybdenum.[4] Zhang, *et al.*, made fracture toughness measurements on sintered Mo-La_2O_3 alloys in 1999. The K_{IC} of the alloy was found to be 2.5 times that of pure molybdenum. Characterization of the microstructure revealed similar grain structures and impurity distribution in both the alloy and the molybdenum, so there was no physical evidence that could help explain the alloy's toughness.[5] Lanthanum oxide has been found to have beneficial effects in

dispersion strengthening of molybdenum; however, the fundamental mechanism responsible for the strengthening of La_2O_3 has still not been identified.

Rare Earth Molybdates

Prior to the study of phase equilibria of systems involving rare-earth oxides and molybdenum, many rare-earth molybdates were synthesized and characterized for the first time in the 1970's. In 1970, Fournier, *et al.,* published a study of the Ln_6MoO_{12} compound containing Y or La as the rare-earth element combined with MoO_3, and also proposed several new compounds, including $La_2Mo_4O_{15}$, $La_2Mo_3O_{12}$, $La_2Mo_2O_9$, La_4MoO_9, $Y_2Mo_4O_{15}$, and Y_6MoO_{12}, based on various stoichiometric values.[6] Brixner, *et al.,* also prepared compounds with rare earth oxides and MoO_3, determining the cell dimensions and space groups for compounds of the form $Ln_2(MoO_4)_3$ where Ln=La, Ce, Pr, Gd, and Sm.[7] They also prepared and determined lattice parameters for Ln_2MoO_6 type rare earth molybdates for Ln= Ce through Lu, Y, and La.[8] In 1977, $LnMoO_5$ compounds, the first identified with a Mo^{IV} valence, were prepared by solid state reaction and by the reduction of Ln_2MoO_6 compounds.[9] Detailed elaboration on these solid-state experimental methods will be given later in this literature review. Kerner-Czeskleba and Tourne published the first analysis of compounds displaying multiple oxidation states of molybdenum in rare-earth molybdates in 1978. In a study using ternary oxides, they found that Mo^{VI} and Mo^{IV} compounds were stable in specific oxygen pressure ranges at high temperatures, and reported that there is also a range of pressures in between where a new type of compound exists in which Mo has a valence of IV or V..[10] They reported that the multiple oxidation states of Mo (IV, V, and VI) can be formed with rare earth oxides, and that these oxidation states can be stabilized so that they will not reduce.[11]

Phase Equilibria Studies

Many studies were done on the phase equilibria of systems containing rare earth oxides and molybdenum oxides. In 1970, with their study of the Ln_6MoO_{12} compounds, Fournier, *et al.,* published preliminary phase diagrams for the La_2O_3-MoO_3 and Y_2O_3-MoO_3 systems. They included in their diagrams many new compounds with varying stoichiometric ratios and provided x-ray diffraction data for several of these compounds.[6] Two years later, Nassau and Shiever studied trivalent tungstates and molybdates of the form $Ln_2(MO_4)_3$. They characterized the phases and determined crystallographic parameters for various lanthanides. Of greater interest were the lanthanide molybdates, which showed more structures than the lanthanide tungstates. Pseudo-binary tungstate-molybdate phase diagrams and structural parameters were given for compounds of La, Nd, Sm, Gd, Ho, and In.[12] In many aspects of its chemical behavior, tungsten is very similar to molybdenum, and the behavior of its compounds can be considered analogous to the behavior of molybdenum compounds. However, for Mo^{IV} compounds this comparison is not as effective because W^{IV} is relatively unstable and readily reduces to (metallic) W.

A phase diagram of the Gd_2O_3-MoO_3 system including $Gd_2(MoO_4)_3$ was published in 1974 using results based on differential thermal analysis and x-ray diffraction. The compound $Gd_2(MoO_4)_3$ was found to melt congruently at its 1:3 stoichiometric ratio of Gd_2O_3:MoO_3. Additional compounds were identified with 1:6, 1:4, and 1:1 Gd_2O_3:MoO_3 ratio compositions.[13]

In 1978, Kerner-Czeskleba, *et al.,* conducted a study of the Ln_2O_3-MoO_2-MoO_3 system at 1473 K for 2:1 Ln:Mo ratio in an attempt to find conditions of stability for

various rare-earth molybdates having different oxidation states of molybdenum. They found that Ln_2MoO_5 (Mo^{IV}) and Ln_2MoO_6 (Mo^{VI}) compounds exist for every Ln at specific oxygen partial pressures. Also, the compounds that were reported as having a Mo valence between IV and VI are only stable in a restricted range of oxygen partial pressures, and do not exist at all for the heavier lanthanides such as Yb or lanthanide-like metals, such as Y. It was concluded that the specific Ln element does affect the oxygen partial pressure range of stability of the molybdates.[10] A later study looked specifically at the lanthanides Pr and Sm between 1000 and 1400 K and oxygen partial pressures between 10^{-6} and 10^{-14} atm. New stable phases were formed; however, the volatility of MoO3 and the unpredictability of the oxidation of Mo made many of the compositions difficult to prepare, so the data is incomplete. Many examples were given of molybdates formed with molar ratios and structures that are similar to those of related rare-earth oxide tungstates.[14] In 1981, phase equilibria in the Nd_2O_3-MoO_2-MoO_3 system were reported between 1273 and 1673 K for O_2 partial pressures between 10^{-5} and 10^{-14} atm. Many stable Mo^{VI} compounds were found on the Nd_2O3-MoO_3 binary, as well as other compounds reported as Mo^{V}. Again, the oxidation of MoO_2 to MoO_3 presented problems in determining the compositions of some phases.[15] Phase equilibria was established in the Ln_2O_3-MoO_2-MoO_3 system for Ln=Gd, Eu, Tb in 1982. New stable compounds were identified in all three systems. It was concluded that the higher the Ln to Mo ratio, the less likely the molybdate phase would be reduced, with the Mo^{VI} compound Ln_6MoO_{12} being the most stable.[16]

Preparation Techniques

In previously reported work, many of the difficulties in experimenting with rare-earth molybdates arose from lack of adequate control in the processing of the materials. As progress was made in the studies of phase equilibria, the preparation techniques were refined and the chemical behavior of the elements was more easily managed. Early processing was done mostly in air. Brixner*, et al.,* described a process of solid-state reaction of the desired rare-earth oxide and MoO_3. A pure MoO_3 powder was produced by decomposition of $(NH_4)_6Mo_7O_{24} \cdot 4H_2O$. Each of the rare-earth oxides was also specially prepared before firing with MoO_3. La_2O_3 was believed to readily absorb water and CO_2 so it was pre-fired in air. Ce_2O_3 was prepared in argon gas or under vacuum to prevent reoxidization to CeO_2. Pr_6O_{11} was used as a starting powder because it easily loses excess oxygen at high temperatures. Stoichiometric mixtures of the powder starting materials were then fired at temperatures up to 1600ºC, in sealed tubes or capsules to control the atmosphere.[7,8]

A publication by Kerner-Czeskleba*, et al.,* described procedures for forming the Mo^{VI} compound Ln_2MoO_6. This procedure noted that MoO_3 should be reduced to Mo in hydrogen prior to reacting, to prevent excessive loss of molybdenum due to evaporation of the volatile MoO_3. Equimolar Ln_2O_3 and Mo were processed in an alumina boat at 1200°C. Pr_2O_3 was obtained by reduction from Pr_6O_{11} as done by Brixner, and Tb_2O_3 was reduced from Tb_4O_7. La_2O_3 powder was used as a starting material and there was no mention of concerns that La_2O_3 absorbs water or CO_2. Although Brixner's concern was valid, no subsequent experiments reported pre-firing the La_2O_3 in air. Partial pressures of O_2 ranged from 10^{-5} to 10^{-13} atm as controlled by appropriate mixtures of CO_2 and H_2 gas

flowing in a horizontal tube furnace.[10] Similar methods were used in later studies of the Ln_2O_3-MoO_2-MoO_3 system for most of the rare-earth oxides.

In the early 1980's, single crystal and oriented polycrystalline samples of rare earth molybdates (La, Nd, Y) with reduced molybdenum complexes were prepared using fused salt electrolysis. These specimens were more appropriate for a variety of characterization techniques. MoO_3 was first calcined in air at 475ºC, and the rare earth oxides were calcined at 1000°C. Stoichiometric mixtures were then weighed out and melted in a crucible. Platinum foil electrodes were used to pass currents through the melt for 30-40 minutes. The electrodes were then removed from the melt and rapidly cooled in air. The cathode would attract the product, separating it chemically and mechanically from the surrounding sample. The desired product grew onto the cathode in the form of prismatic crystals.[17] This technique was also later used to prepare $La_2Mo^{IV}{}_2O_7$ for an analysis of electrical, magnetic, and structural properties and to compare it with other rare-earth molybdates having the $Ln_2Mo_2O_7$ formula.[18]

A precipitation method was developed by Huang, *et al.,* to prepare $Ln_2(MoO_4)_3$. First, the rare-earth oxide was dissolved in HNO_3, and then mixed with an ammonium paramolybdate solution. The paramolybdate can be added in excess, as its amount does not affect the composition of the rare-earth molybdate formed. They then added NH_4OH to the solution to control the pH between 5.5 and 7 while the precipitate formed. The precipitate was then filtered, washed, and dried at 120ºC. The precipitate was calcined in air at 520ºC to yield the molybdate.[19]

The La_2O_3-MoO_3 System

The first projected phase diagram for the La_2O_3-MoO_3 system, shown in Figure 2.1, was published in 1970.[20] By experimenting with various molar ratios of La_2O_3 to MoO_3, new compounds were produced and they were characterized using x-ray diffraction. At the 1:4 ratio, tetragonal $La_2Mo_4O_{15}$ was reported, along with 1:3 monoclinic $La_2Mo_3O_{12}$, 1:2 cubic $La_2Mo_2O_9$, and 1:1 tetragonal La_2MoO_6. [6]

Over the following years, researchers discovered new compounds in this system that were missing from the preliminary phase diagram. Alekseev, *et al.,* reported the 2:1 compound La_4MoO_9 and found that it had a hexagonal structure.[21] In 1972, the 3:1 compound La_6MoO_{12} was produced and characterized as cubic.[22] Kerner-Czeskleba and Cros synthesized and characterized two new compounds: the FCC pyrochlore $La_{10}Mo_2O_{21}$ with a 5:2 molar ratio, and orthorhombic $La_6Mo_2O_{15}$ with a 3:2 molar ratio. They also reevaluated the crystal structure of La_6MoO_{12} and reported it as rhombohedral[23]

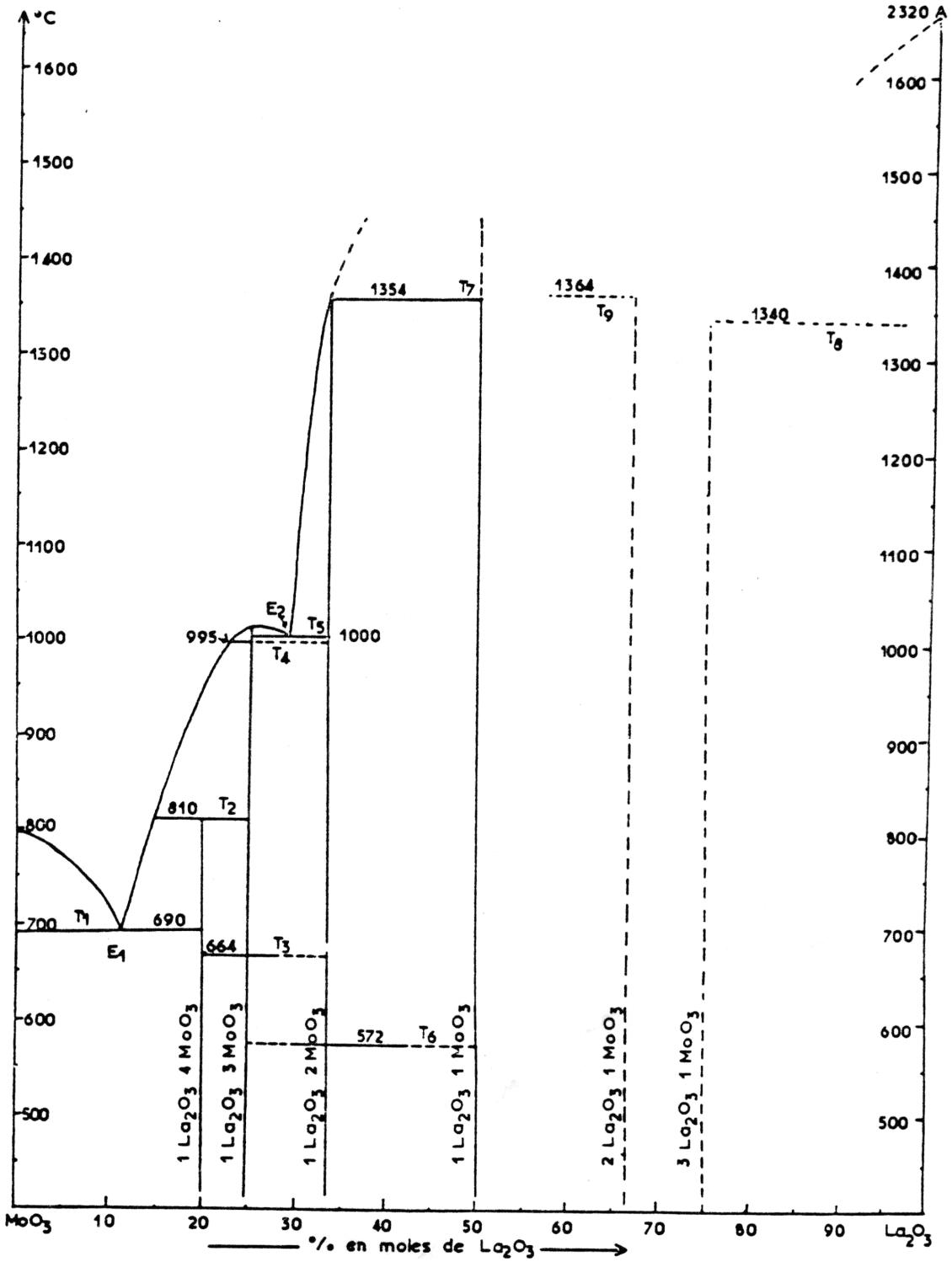

Figure 2.1 MoO_3-La_2O_3 Phase Diagram

The La_2O_3-MoO_2 System

Due to the instability of the Mo^{IV} oxide MoO_2 at atmospheric oxygen pressure conditions, there have not been any published phase diagrams for the La_2O_3-MoO_2 system. The first compound reported in this system was La_2MoO_5, produced by Hubert from equimolar La_2O_3 and MoO_2.[9] This same compound was synthesized later by Kerner-Czeskleba and Tourne who determined it was monoclinic.[10] Years later, the crystal structure was revised to cubic after an x-ray diffraction study.[24] Hubert also reported a 2:1 molar compound, La_4MoO_8, with x-ray diffraction data, but no evaluation of crystal structure.[25] In 1987, an orthorhombic compound, $La_2Mo_2O_7$ was prepared with a 1:2 molar ratio of La_2O_3 and MoO_2. Synthesis was performed using both fused salt electrolysis and solid-state reaction.[18]

The La_2O_3-MoO_2-MoO_3 System

Several compounds have been recognized as forming from a mixture of molybdenum valences, positioning them in the La_2O_3-MoO_2-MoO_3 system. Hubert reported mixed-valence compounds that he produced by solid-state reaction of stoichiometric mixtures of La_2O_3, MoO_2, and MoO_3 powder. He synthesized the 3:4 molar La_2O_3:MoO_x compound $La_3Mo_2O_9$. For this compound, a 4:5 molar mixture of La_2O_3:MoO_2 was heated to 1250ºC in argon.[26] He also produced another 3:4 La_2O_3:MoO_x compound, $La_3Mo_2O_{10}$, by heating a mixture of La_2O_3, MoO_2, and MoO_3 to 1250ºC in argon.[27] The cubic 5:6 $La_5Mo_3O_{16}$ compound was later prepared by heating the powder constituents (La_2O_3, MoO_2, and MoO_3) above 1200ºC under vacuum.[28] Kerner-Czeskleba*, et al.,* later did extensive work in a number of Ln_2O_3-MoO_2-MoO_3 systems with La and several other rare-earth elements. All samples were produced using

solid-state reaction of powders in an atmosphere of controlled oxygen partial pressure. In their experiments, they were unable to reproduce any of Hubert's compounds but they discovered and characterized new compounds. In their investigation of stable phases with a 1:1 La_2O_3:MoO_x molar ratio, they found $La_{12}Mo_6O_{35}$ forming at partial pressures between those defining the limits of stability of La_2MoO_5 and La_2MoO_6. They accounted for the resulting molybdenum oxidation number as two Mo^V for four Mo^{VI}.[10] A subsequent publication assigned the orthorhombic crystal structure to $La_{12}Mo_6O_{35}$ using x-ray diffraction data.[11] There was no evidence of Hubert's $La_5Mo_3O_{16}$ or $La_7Mo_4O_{22}$.[28] The 3:2 compound $La_6Mo_2O_{14}$ was synthesized that same year and reported to be hexagonal.[23]

In 1992, Gall and Gougeon produced $La_4Mo_2O_{11}$ using a 1:1 molar ratio of La_2O_3:MoO_x. It was formed by heating La_2O_3, MoO_3, and Mo in sealed molybdenum crucibles to 1980 K. They proposed a tetragonal crystal structure, based on the presence of a Mo_2O_{10} dimeric unit because they felt that $La_4Mo_2O_{11}$ was analogous to the established structure of $Nd_4Re_2O_{11}$. It is known that rhenium can form mixed valence oxides such as this with Re-Re dimers and Re_2O_{10} groups that can link to each other in a Re-O network that allows for electron delocalization. The behavior of molybdenum is not understood this well. XRD data was on file for $La_4Mo_2O_{11}$ with the ICSD, but not published in the journal article.[29]

The Y_2O_3-MoO_x System

The Y^{3+} ion is similar to the La^{3+} ion in radius, so yttrium molybdates have often been studied along with the lanthanum molybdates in many of the same experiments. Several yttrium molybdates have been identified with a molybdenum valence of 6;

however, very few have been found with a valence of 4 in comparison to the variety of lanthanum molybdates that have been discovered for both oxidation states of molybdenum.

Along with their diagram for the La_2O_3-MoO_3 system, Fournier, *et al.,* also published a preliminary phase diagram for Y_2O3-MoO_3, shown in Figure 2.2. Samples were prepared by mixing specific molar ratios of Y_2O_3 with MoO_3 and pressing them into pellets. The pellets were then reacted at temperatures up to 1500ºC, in an unspecified atmosphere. $Y_2Mo_4O_{15}$ was formed from a 1:4 molar ratio and found to be stable up to 830ºC. Also, 1:3 molar $Y_2Mo_3O_{12}$ and equimolar Y_2MoO_6 were reported stable up to 1310ºC. Crystal structures could not be established for these phases in the molybdenum-rich portion of the phase diagram. A 2:1 Y_4MoO_9 compound was formed at 1400ºC and determined to be hexagonal. Also, a 3:1 Y_6MoO_{12} compound was found to be hexagonal at low temperatures, while forming a new high temperature FCC phase at 1500ºC. X-ray diffraction data and crystallography information was published for the Y_2O_3-rich phases.[6] Experiments conducted by Kerner-Czeskleba, *et al.,* attempted to form an equimolar Y_2O_3-MoO_x mixed valence compound between Y_2MoO_5 and Y_2MoO_6 over a range of oxygen partial pressures. The study concluded that there is a direct transition from the Mo^{IV} compound to the Mo^{VI} compound with no mixed-valence compound forming.[10]

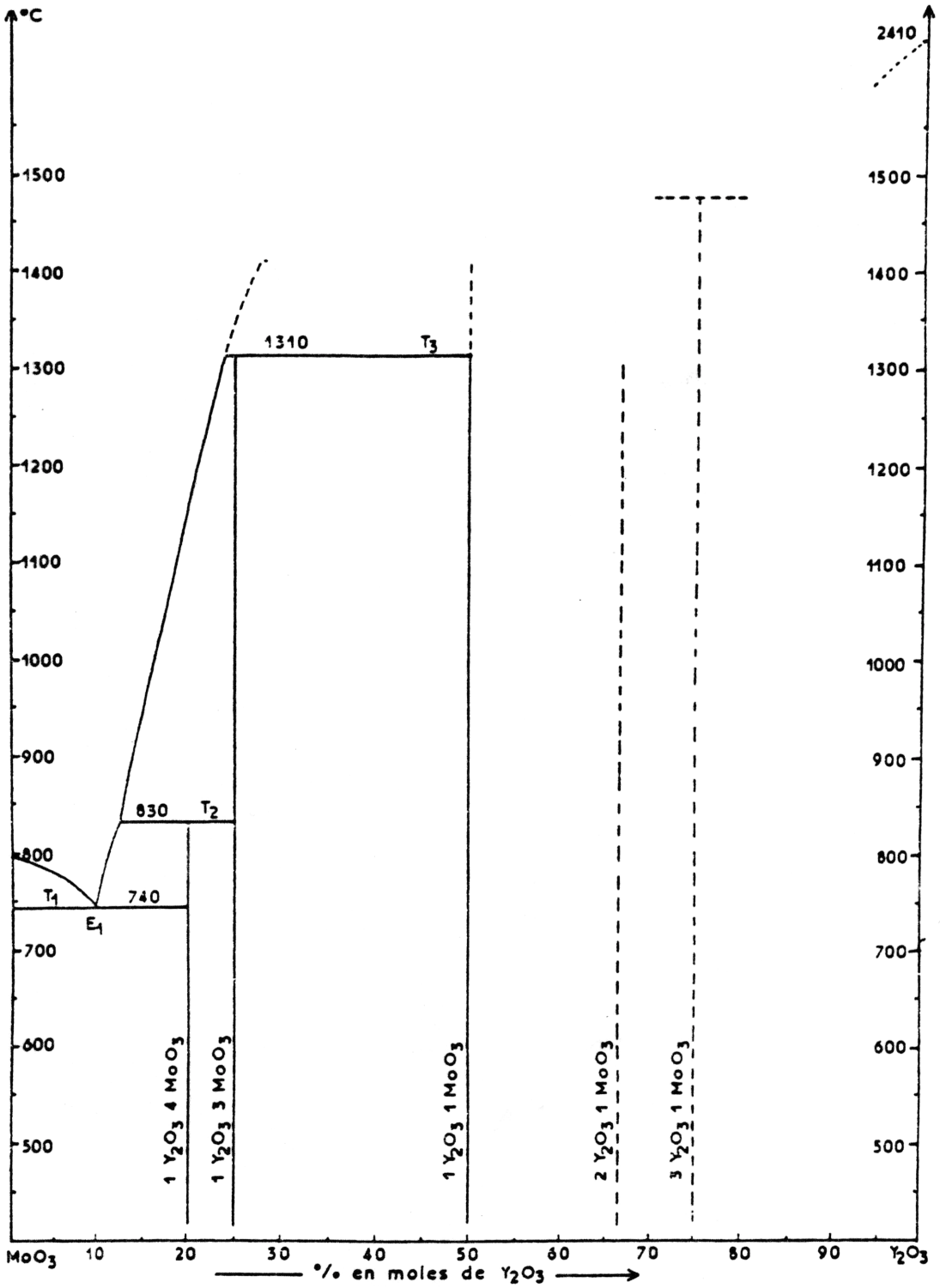

Figure 2.2 MoO_3-Y_2O_3 Phase Diagram

Riemers, *et al.*, synthesized a Mo^{IV} compound, $Y_2Mo_2O_7$, using a 1:2 molar mixture of Y_2O_3 and MoO_2 in 1988. Powder neutron diffraction data was used to determine the crystal structure as cubic pyrochlore. Bond distances were found to be in excellent agreement when compared to similar compounds such as $Y_2Ti_2O_7$ and $Y_2Sn_2O_7$.[30]

In 1985, $Y_5Mo_2O_{12}$ was synthesized via electrochemical reduction of alkali-molybdates, MoO_3, and rare-earth oxides by Torardi, *et al*. Their study initally aimed to use fused salt electrolysis to synthesize the Y_2MoO_5 compound previously reported by Hubert[9] and Kerner-Czeskleba.[10] The method enabled them to produce single crystals, which allowed for detailed diffraction studies. Crystal diffraction analysis of Y_2MoO_5 revealed that the unit cell actually contained 10 Y atoms and 4 Mo atoms, yielding the chemical formula $Y_5Mo_2O_{12}$. Supporting electrical and magnetic data were published for this compound as well as for $Gd_5Mo_2O_{12}$. No other rare-earth molybdates of this $Ln_5Mo_2O_{12}$ form were synthesized in the study. $Y_5Mo_2O_{12}$ was found to have an average Mo oxidation of 4.5, making it the first yttrium molybdate reported to have a mixed molybdenum valence.[31]

A study in 1994 of the Y_2O_3-MoO_x system investigated the synthesis of a new yttrium molybdate with a molybdenum valence less than six. Researchers began by preparing $YMoO_4$ (1:2 Y_2O_3:MoO_3, average Mo valence of 5) by solid-state reaction of Y_2O_3 and MoO_3 at 1200ºC. After careful analysis using x-ray diffraction and electron microscopy, they determined that there were two phases present with the yttrium-molybdenum ratios of 1:3 and 5:8. The $YMoO_4$ composition now appeared to consist of a binary mixture of $Y_5Mo_4O_{18}$ (5 Mo^{VI} – 3 Mo^{IV}) and $Y_2Mo_3O_{10}$ (2 Mo^{VI} – 4 Mo^{IV}). The

researchers were able to isolate the compound believed to be $Y_5Mo_4O_{18}$ and determined its atomic structure and parameters. No confirmation could be made of the exact formula of the other compound, assumed to be $Y_2Mo_3O_{10}$.[32]

The ZrO_2-MoO_x System

A study of the zirconia-molybdenum oxide system provides a good example for future work supplementing that on the lanthanide molybdates. The zirconia system involves a tetravalent metal for comparison with the yttrium oxide and lanthanide oxide systems, which are trivalent. The existence of a mixed molybdenum valence zirconium molybdate could provide insight into the impact of cation crystallography on behavior of the molybdate. The first reported zirconium molybdate was prepared in 1967 when Trunov and Kovba produced a single crystal of $ZrMo_2O_8$ and published its x-ray diffraction data.[33] The same compound has also been labeled $Zr(MoO_4)_2$ and is a Mo^{VI} compound that crystallizes in two phases: a low temperature one and a high temperature one that exists above 913 K. Its composition and structure have been reported, verified by x-ray diffraction and vibrational spectroscopy.[34] The crystallography of the high temperature form was later re-examined and a new crystal structure was given with atomic parameters. $Zr(MoO_4)_2$ was synthesized by heating a 1:2 stoichiometric mixture of ZrO_2 and MoO_3 powder to 1123 K and then quenching to prevent any transition to the low-temperature form.[35]

There is very limited information on zirconium molybdates, and so far no mixed molybdenum valence compounds have been reported. One related study of phase equilibria was done in 1962 on the quaternary system, Mo-Ti-Zr-O. Powders were reacted in a vacuum furnace at 1500ºC and characterized by x-ray diffraction. The

quaaternary system was presented as a tetrahedron, on which the triangular faces represented isothermal ternary systems. Experiments were run at many different conditions, and regions were recognized as single or multi-phase; however, the actual composition and formula of these phases were not identified.[36]

The CeO_2-MoO_x System

CeO_2 is another rare-earth oxide that reacts with molybdenum in similar ways to La_2O_3 and Y_2O_3. Many of the studies of rare-earth molybdates include cerium molybdates. Although difficult to work with due to variation of cerium oxidation states, they have been of great interest due to the many applications of cerium, such as refractory materials, luminescence, or catalysis. In 1972, two studies published by Brixner, *et al.*, involved synthesis and crystallographic analysis of cerium molybdates. They prepared Ce_2MoO_6 by combining CeO_2, Mo, and MoO_3 powder in a molar ratio of 6:1:2. This powder mixture was pressed into a pellet and sintered in a sealed Pt capsule between 1400 and 1600ºC. Their discussion of the valence states in Ce_2MoO_6 concluded that both Ce^{III} and Ce^{IV} were present and that Mo had reduced from Mo^{VI} to Mo^{V} during the reaction.[8] Solid-state reaction was also used to prepare $Ce_2(MoO_4)_3$, from CeO_2 and MoO_3 powder starting materials.[7] Also in the CeO_2-MoO_3 system, $CeMo_2O_8$ and $Ce_2Mo_3O_{13}$ have been produced and characterized.[37] Bart and Giordano published a study of phase relationships in the cerium-molybdenum oxide system in 1975. $Ce_2Mo_4O_{15}$ was prepared by adding $(NH_4)_6Mo_7O_{24}{\cdot}4H_2O$ to $Ce(NO_3)_3{\cdot}6H_2O$ in various Ce-Mo ratios, drying the samples, and calcining them in air at 500 to 800ºC. The same compound was also synthesized by calcining CeO_2, MoO_3, and MoO_2 at 550ºC. A high temperature compound α-$Ce_2Mo_3O_{13}$ and lower temperature compounds β-$Ce_2Mo_3O_{13}$

and $Ce_2Mo_3O_{12.25}$ were prepared via solid-state reaction of CeO_2 and MoO_3 in He or air. Phase transformation temperatures between all of these phases were established and part of the equilibrium phase diagram of the Ce_2O_3-MoO_3 system was presented.[38] This phase diagram agreed well with the phase diagram for the La_2O_3-MoO_3 system published in 1970 by Fourier, *et al.*[6]

CHAPTER 3

EXPERIMENTAL PROCEDURE

The samples used in this study were all produced using solid-state processing of powder starting materials. Experiments were targeted towards forming molybdates at reduced oxygen partial pressures and high temperatures. Powders were heated to reaction temperature in a horizontal tube furnace under a controlled atmosphere. A combined flow of H_2 and CO_2 gas provided control of the oxygen partial pressure inside the system. After preparation, the samples were characterized using x-ray diffraction to determine the phases that had formed.

Preparation and Processing of Samples

All samples were prepared using powder starting materials of Mo (H. C. Starck, <10μm, Stock # 46838) combined in stoichiometric ratios with La_2O_3 (Alfa Aesar, 99.99% pure, <10μm, Stock # 11264), Y_2O_3 (Alfa Aesar, 99.99% pure, <10μm, Stock # 11180), or ZrO_2 (Zirconia Sales (America), Inc., 99.7% pure, <5μm, Grade DK3-CL). Samples of approximately 0.5 cm^3 were produced to guarantee enough product to use in an x-ray diffractometer. All weight measurements were made to four significant figures using a Mettler AE50 Analytical Balance. Powders were mixed by grinding with a mortar and pestle until the sample was uniform in color. The sample was packed into an alumina crucible and compressed with a stainless steel rod.

A shallow rectangular alumina boat was used to hold the crucibles while they were heated in the furnace. As many as four samples in crucibles could be processed during one trial. During the experiments, the samples were heated to 1000 or 1200

degrees C. All samples were kept at the reaction temperature for at least 48 hours to ensure completion of the reaction. The oxygen partial pressure was also controlled to a pressure between 10^{-10} Pa and 10^{-5} Pa during the reaction by establishment and maintenance of the appropriate CO_2:H_2 ratio.

Experimental Setup

A process flow diagram of the experimental apparatus is shown in Figure 3.1. The components of this diagram will be explained in detail later in this chapter.

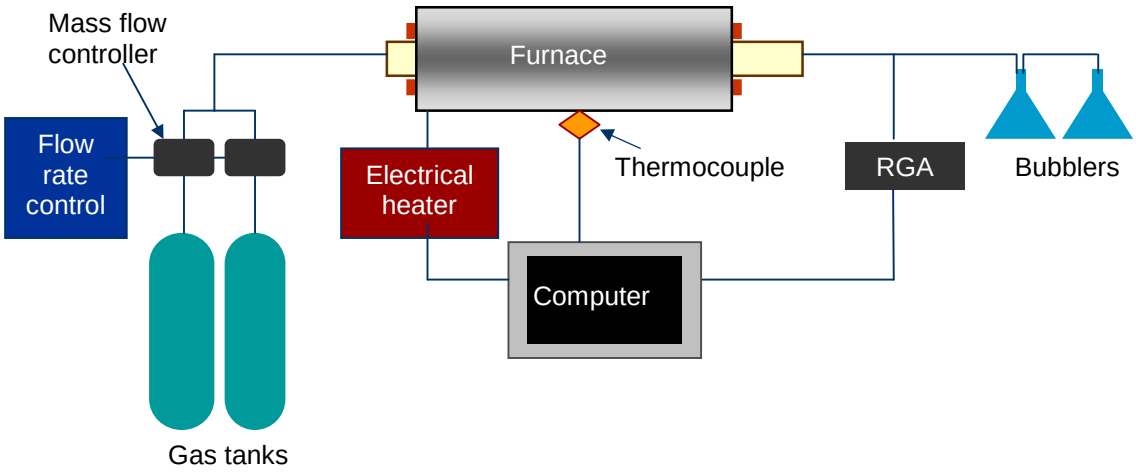

Figure 3.1 Process Flow Diagram

The body of the furnace consisted of a 2.75-inch diameter mullite tube obtained from Harrop Laboratories with 14 Globar silicon carbide heating elements running parallel to the tube evenly distributed around the outside. Figure 3.2 shows the exterior of the tube furnace.

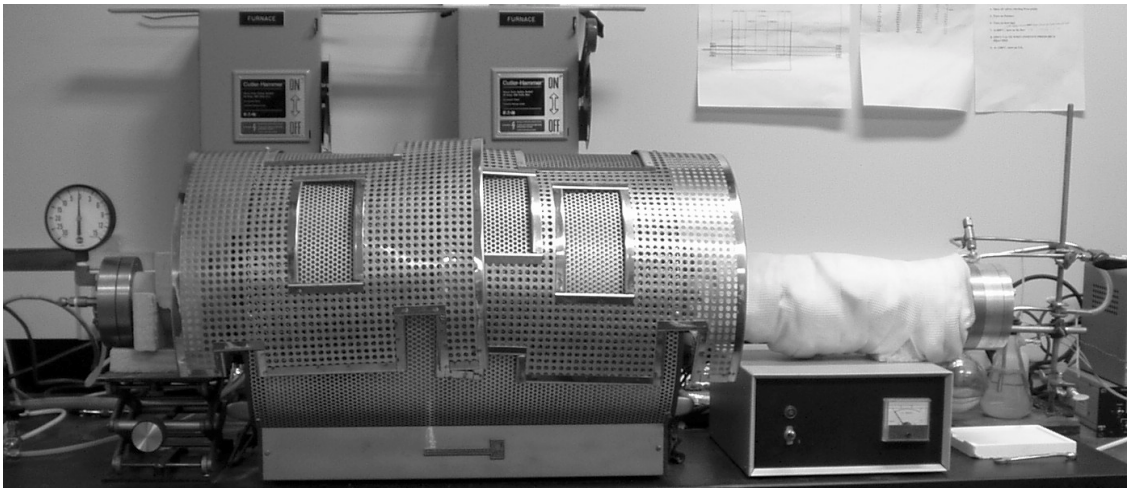

Figure 3.2 Tube Furnace Used for Heating Samples

Circular steel end plates were fastened onto the ends of the mullite tube using 3 bolt clamps to retain each plate. A pressure gauge attached to the inlet end plate indicated the equilibrium pressure inside the tube. Vacuum grease was applied to a rubber o-ring which was embedded into the end of the furnace tube to create an airtight seal. These end plates, seen in Figure 3.3 and Figure 3.4, contained airtight fittings for the gas delivery and exhaust tubing.

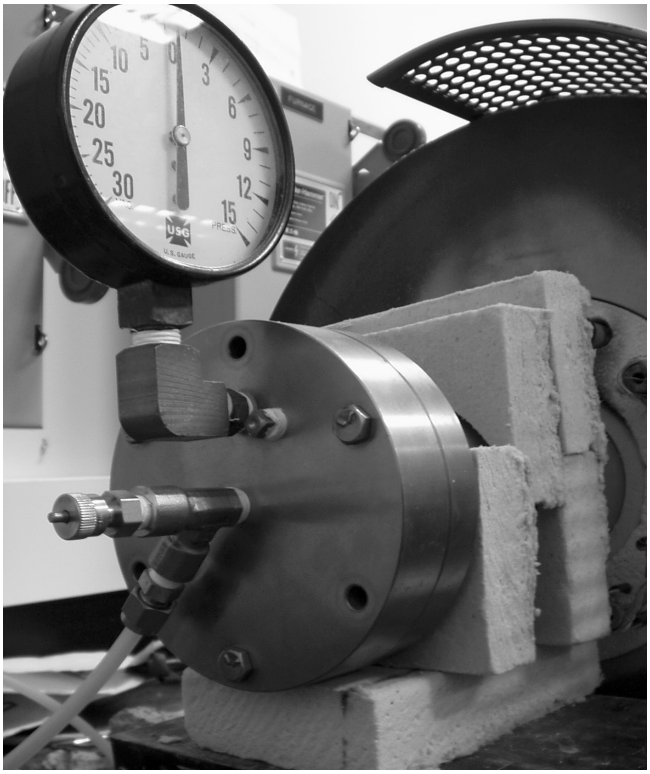

Figure 3.3 End Plate at Inlet of Furnace Tube with Pressure Gauge

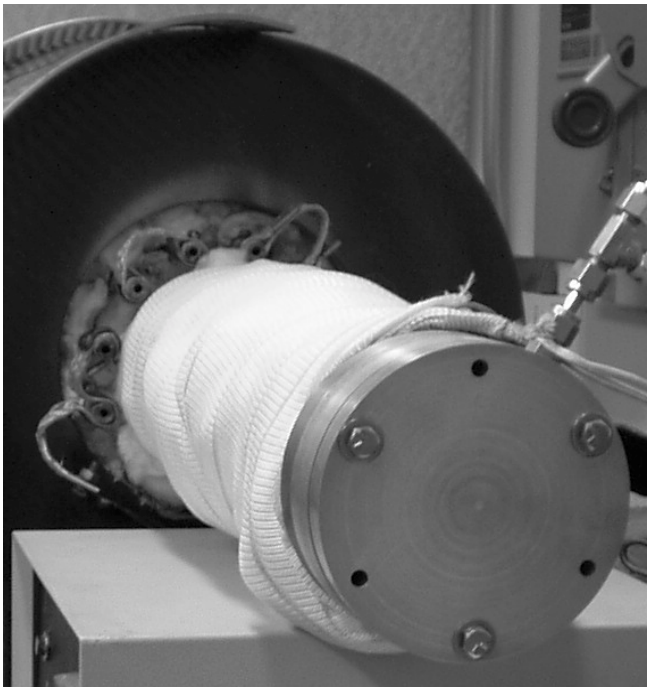

Figure 3.4 End Plate at the Outlet of the Furnace Tube

Within the tube, the samples were held in a rectangular alumina boat. This boat was enclosed on either end by cylindrical heat shields manufactured from refractory brick. The inner faces of these heat shields were coated with alumina to provide reflection of heat inward. Heat tape, refractory brick, and insulation were added on the outside of the furnace tube to minimize heat loss. A schematic of the furnace and its inner parts is shown in Figure 3.5.

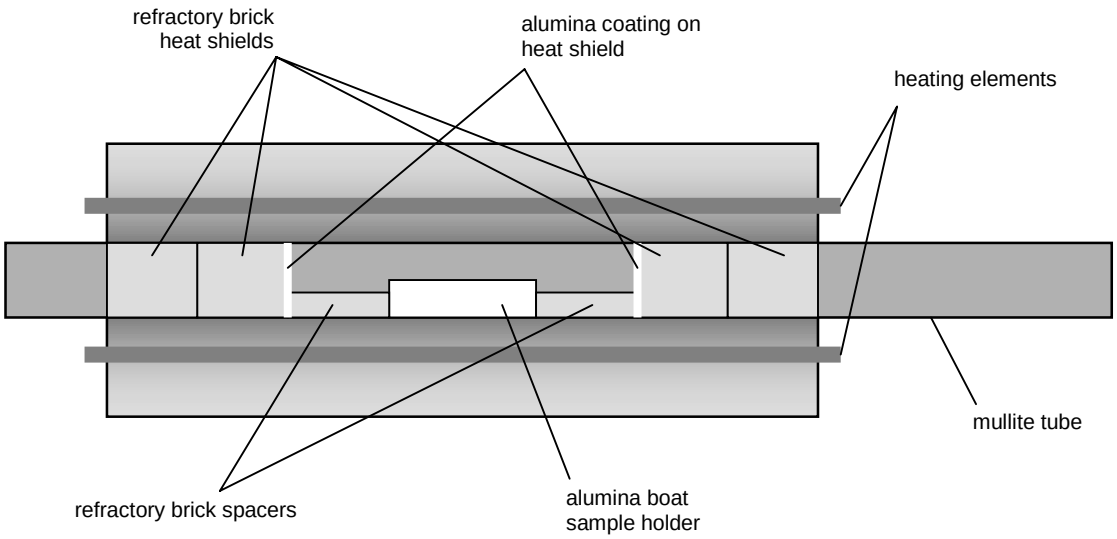

Figure 3.4 Cross-sectional Schematic of Furnace

Temperature Control

The heating elements in the furnace had the capacity to heat samples up to 1450 degrees C. A Type-S platinum/platinum-rhodium thermocouple was placed near the (axial) center of the furnace on the outside of the tube to monitor the temperature. Inside the tube, a Type-K chromel-alumel thermocouple was placed and used along with the Type-S thermocouple to calibrate the furnace temperature. It was determined that near

constant temperature was maintained over a length of about 4 inches. Samples in the boat were pushed into the center of this 4-inch area during each trial. Heating schedules were set using computer software that allows one to establish heating rates, temperatures, and periods to be held at a constant temperature. The heating and cooling rates for experiments run up to 1200°C are provided in Table 3.1.

Table 3.1 Heating and cooling rates for furnace

Rate (ºC/min)	**Final Temperature (ºC)**
5 (heating)	1200
10 (cooling)	1000
5 (cooling)	500
2 (cooling)	200

Atmosphere Control

The atmosphere in the furnace was controlled using a combined flow of hydrogen and carbon dioxide gas. Gas was obtained from Airgas of ultra high purity. Thermodynamic calculations, included in Appendix A, were made to determine the combination of gas flow rates necessary to produce the desired oxygen partial pressures inside the furnace at each temperature. The plot in Figure 3.6 shows the variation of partial pressure of O_2 with the ratio of CO_2 to H_2 gas.

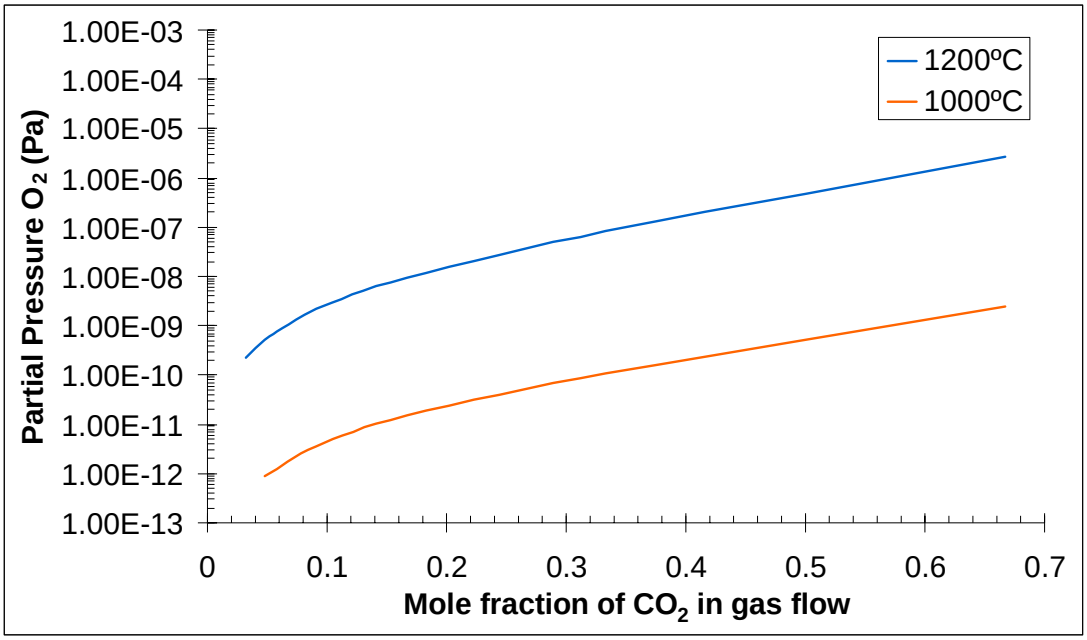

Figure 3.6 Partial pressure of O_2 vs. fraction of CO_2 in the gas flow

A Visual Basic program was written to calculate the molar ratio of gases necessary to achieve the desired O_2 partial pressure at a given temperature. The program code is included in Appendix B. The desired molar ratios of CO_2 and H_2 were used to determine corresponding volumetric flow rates. A combined gas flow rate of approximately 120 cc/min was maintained. Flow rate control was provided by MKS mass flow and an MKS model 247C controller to control the actual flow rates.

Gases from the supply tanks were fed to the furnace through polyethylene tubes on the inlet end, and flowed out of the system through stainless steel tubing at the exhaust end. The outlet tubing was connected through one flask to a bubbler into a second flask to avoid drawing air or moisture into the system in the event that a vacuum was created. All of the experiments were started in pure H_2 until the furnace approached 800 degrees C to allow water or organics to decompose, and to prevent the formation of

molybdenum oxide or molybdenum carbide from the CO_2. At 800 degrees, the CO_2 was added at a flow rate that corresponded to the desired gas proportions.

A residual gas analyzer (RGA) was also connected to the furnace to monitor the gas species in the system. The resulting RGA spectra were monitored in real time using TWare32 Process Gas Characterization Software. This data was useful for detecting leaks and monitoring gas equilibrium during furnace runs.

Characterization

X-ray diffraction (XRD) was used to characterize the phases present in the processed samples. After firing in the furnace, the samples were removed and extracted from the crucibles. Oftentimes the samples would emerge slightly sintered, so they were always ground into a fine powder using a mortar and pestle. The resulting powder was packed into a metal diffraction sample holder using a glass slide as a smooth packing surface. A Philips automated powder diffractometer (PW 1800) was used to collect x-ray diffraction data over a range of 10 to 90 degrees 2θ. Data acquisition was performed using the Philips PW-1877 Automated Powder Diffraction program (version 3.6). After the scan was complete, the raw data files were examined for clarity and intensity and a peak search was performed. Any phases present were identified using the PW1876 PC-Identify program (version 1.0) in conjunction with the JCPDS Powder Diffraction File database. In the PC-Identify program, restriction files were created to limit the identified patterns to ones containing only the elements known to be present in the sample.

CHAPTER 4

RESULTS AND DISCUSSION

This chapter presents the phase equilibria results obtained from the experiments and characterized by x-ray diffraction. All of the phases identified are presented in tables with the corresponding experimental conditions. X-ray diffraction data are also included for all of the phases discussed.

The lanthanum-molybdenum oxide experiments at 1000°C and 1200°C yielded enough conclusive data to construct isothermal phase diagrams. Compounds observed in this system are plotted on a chart of oxygen partial pressure versus composition for each reaction temperature. The relevant x-ray diffraction patterns are included as evidence for the phases shown in the diagram. Results from the experiments with yttrium and zirconium are also presented and discussed with supporting x-ray diffraction patterns.

The specific compounds formed by reaction of rare-earth oxides with molybdenum are dependent on the extent to which molybdenum oxidizes in the controlled oxygen partial pressure atmosphere. As oxygen is added, Mo will form MoO_2, with a molybdenum valence of IV, and in the presence of additional oxygen, some fraction of the Mo will form MoO_3, with a molybdenum valence of VI. For that reason the data for each system are discussed in segments according to the partial pressure of oxygen during the reaction. In some of the preceding literature, rare-earth molybdates have been described as having molybdenum valences of IV, V, and VI. The Mo^V compounds published to date have not been well supported with structural or

experimental data. As a result, any compound having a molybdenum valence between IV and VI is depicted in this study as a mixed valence compound of Mo^{IV} and Mo^{VI}.

$LaO_{1.5}$-MoO_x system at 1200°C

Phase identification was performed using the PC Identify software for all of the samples prepared in the $LaO_{1.5}$-MoO_x system. Resulting phases, experimental conditions, and the percent of molybdenum in the sample are given in Table 4.1 tabulating the results at 1200°C in order of decreasing pO_2 values and decreasing La:Mo ratio for each pO_2 value. Primary phases for each processed sample are indicated by bold type. Phases identified here were used to construct the binary phase diagram seen in Figure 4.1. The x-axis represents the molar percent of molybdenum or molybdenum oxide in the sample, and the y-axis is a log scale of the oxygen partial pressure at which the phases form. Lines are drawn in to represent stable compounds that were determined by experiments or identified from the literature. As seen in Table 4.1, several samples were found to have more than two phases present after processing. In some cases, the additional phases might be intermediate reaction products indicating that the sample had not attained equilibrium. The existence of three or more phases at equilibrium also suggests that the $LaO_{1.5}$-MoO_x system would be better presented as the La-Mo-O ternary system, and that the binary presented is a section of a ternary phase diagram. For this study; however, it will be assumed that the binary presentatation of Figure 4.1 is a sufficient representation of the data.

Table 4.1 Phases identified from experiments with La_2O_3 and Mo at 1200°C

Sample Name	La:Mo Ratio	Molar % Mo	O_2 Partial Pressure (Pa)	Process Time (hours)	Phases Present
LAMO_02	2:1	33.33	2.645E-06	50	**La_2MoO_6**
LAMO_53	11.33:1	8.11	4.641E-07	60	**La_2O_3**, unable to identify, La_6MoO_{12}
LAMO_55	3.71:1	21.21	4.641E-07	60	**$La_6Mo_2O_{14}$**, La_2MoO_5
LAMO_10	2:1	33.33	4.641E-07	51	**$La_{12}Mo_6O_{35}$**, $La_6Mo_2O_{14}$, $La_5Mo_3O_{16}$
LAMO_54	1.33:1	42.86	4.641E-07	60	**$La_{12}Mo_6O_{35}$,** $La_5Mo_3O_{16}$, $La_5Mo_4O_{14}$, $La_2Mo_2O_7$
LAMO_60	3:1	25.00	1.976E-07	60	**$La_6Mo_2O_{14}$,** $La_{10}Mo_4O_{24}$, $La_4Mo_2O_{11}$
LAMO_61	2:1	33.33	1.976E-07	60	**$La_4Mo_2O_{11}$**
LAMO_62	1:1.5	60.00	1.976E-07	60	$La_2Mo_3O_{10}$
LAMO_57	6:1	14.29	8.147E-08	60	**$La_6Mo_2O_{14}$,** La_2O_3, La_2MoO_5
LAMO_34	2:1	33.33	8.147E-08	50	**$La_{10}Mo_4O_{24}$**, $La_2Mo_3O_{10}$
LAMO_58	1.08:1	48.15	8.147E-08	60	**$La_{10}Mo_4O_{24}$,** $La_2Mo_3O_{10}$
LAMO_59	1:1.5	60.00	8.147E-08	60	$La_2Mo_3O_{10}$
LAMO_33	1:4.5	81.82	8.147E-08	50	**Mo**, unable to identify
LAMO_33B	1:4.5	81.82	8.147E-08	50	**Mo**, unable to identify
LAMO_66	1:1.5	60.00	1.601E-08	60	**Mo,** $La_2Mo_3O_{10}$, $La_{10}Mo_4O_{24}$
LAMO_67	1:2	66.67	1.601E-08	60	**Mo,** $La_2Mo_3O_{10}$
LAMO_35	6:1	14.29	9.697E-09	50	**$La_6Mo_2O_{14}$**, La_2O_3, La_2MoO_5
LAMO_32	2:1	33.33	9.697E-09	50	**$La_{10}Mo_4O_{24}$**
LAMO_32B	2:1	33.33	9.697E-09	50	**$La_{10}Mo_4O_{24}$**
LAMO_36	1.33:1	42.86	9.697E-09	50	**$La_{10}Mo_4O_{24}$,** $La_2Mo_3O_{10}$
LAMO_63	1.33:1	42.86	9.697E-09	70	**$La_{10}Mo_4O_{24}$,** $La_2Mo_3O_{10}$
LAMO_64	1:1.5	60.00	9.697E-09	70	**Mo,** $La_2Mo_3O_{10}$, $La_{10}Mo_4O_{24}$
LAMO_65	1:2	66.67	9.697E-09	70	**Mo,** $La_2Mo_3O_{10}$
LAMO_31	1:4.5	81.82	9.697E-09	50	**Mo,** $La_2Mo_3O_{10}$
LAMO_31B	1:4.5	81.82	9.697E-09	50	**Mo,** $La_2Mo_3O_{10}$
LAMO_20	2:1	33.33	2.168E-09	96	**$La_{10}Mo_4O_{24}$**
LAMO_30	1:4.5	81.82	2.168E-09	50	**Mo,** $La_{10}Mo_4O_{24}$
LAMO_30B	1:4.5	81.82	2.168E-09	50	**Mo,** $La_{10}Mo_4O_{24}$
LAMO_02B	2:1	33.33	2.239E-10	68	**La_2O_3,** Mo

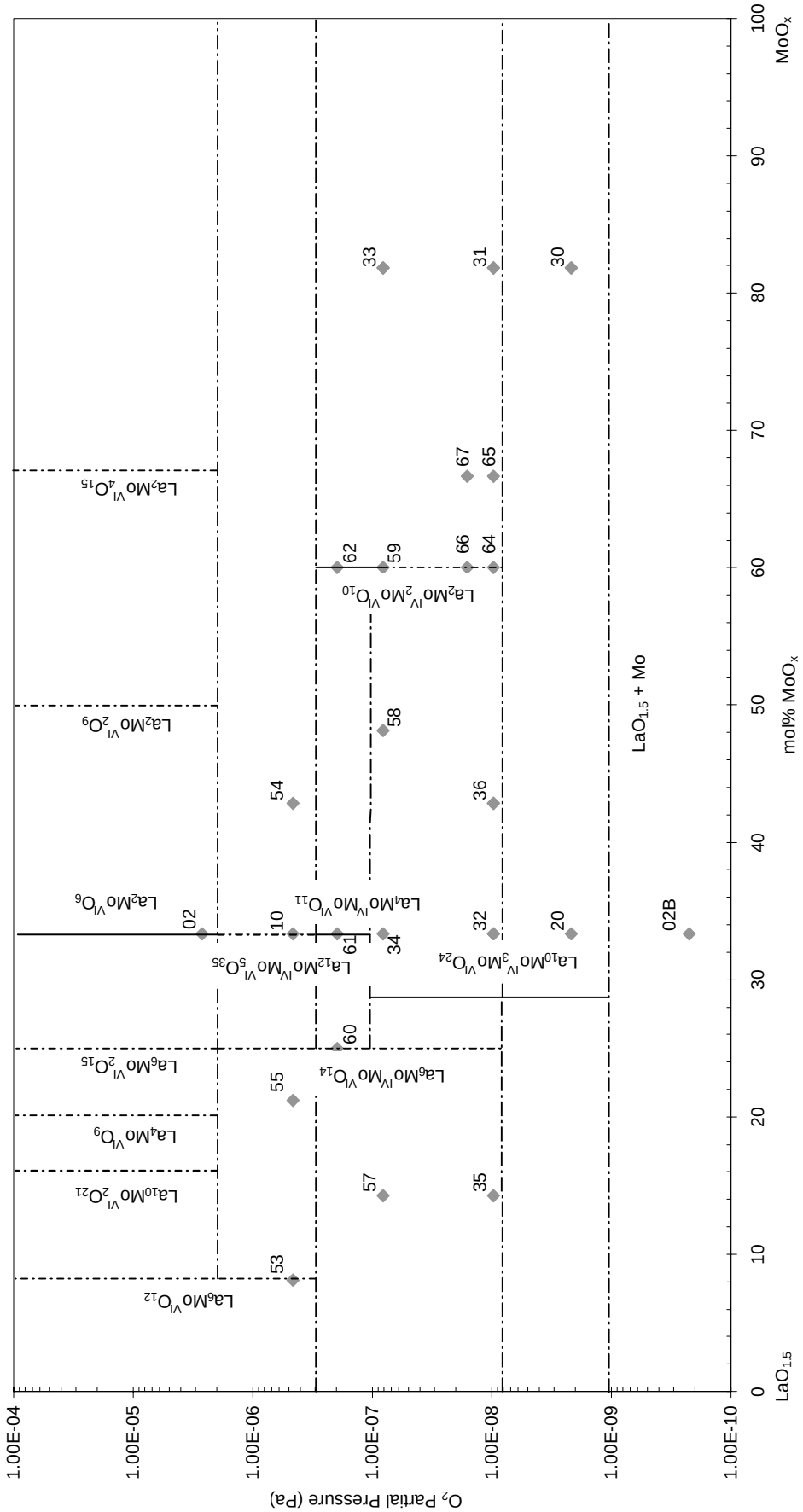

Figure 4.1 Phase equilibria in the $LaO_{1.5}$-MoO_x system at 1200ºC

Oxygen Partial Pressures from $1x10^{-4}$ to $2x10^{-6}$ Pa

Compounds formed in this region have a molybdenum valence of VI. The following compounds have been reported in the literature as stable Mo^{VI} compounds depending on the La-Mo ratio: La_6MoO_{12}, $La_{10}Mo_2O_{21}$, $La_6Mo_2O_{15}$, La_4MoO_9, La_2MoO_6, $La_2Mo_2O_9$, and $La_2Mo_4O_{15}$.[22,21,8,6] Previous work done in this system verified the existence of all of these phases in this pressure range; however, the lower O_2 partial pressure limit could not be confirmed. The only sample formed as a pure phase in this work was La_2MoO_6 using a 2:1 molar ratio of La to Mo. La_2MoO_6 was found to be stable at oxygen partial pressures as low as $2.645x10^{-6}$ Pa, therefore this is set as the stability limit of the Mo^{VI} compounds for compounds with MoO_x greaater than approximately 10 mole percent.

Oxygen Partial Pressures from $2x10^{-6}$ to $3x10^{-7}$ Pa

At 1200ºC in this pressure range, molybdenum begins to form mixed-valence compounds. The x-ray diffraction pattern for sample LAMO_53, which was formed from approximately 8.11% Mo at an O_2 partial pressure of $4.6x10^{-7}$ Pa, is seen in Figure 4.2. The peak sizes show a small amount of the Mo^{VI} phase La_6MoO_{12}, but none of the other Mo^{VI} compounds could be synthesized in this pressure range. As reported in the review of literature, Prevost-Czeskleba and Tourne[16] found that compounds with a molybdenum valence of VI are less likely to be reduced as the concentration of Mo decreases, with compounds of the form Ln_6MoO_{12} being the most stable. For this reason, the stability limit for Mo^{VI} compounds is inferred to be an O_2 partial pressure of $3x10^{-7}$ Pa for Mo concentrations less than approximately eight to ten mole percent.

The sample run using a 3.71:1 La:Mo ratio at an oxygen partial pressure of $4.6x10^{-7}$ Pa (LAMO_55) was found to contain primarily $La_6Mo_2O_{14}$, which is a mixed-molybdenum valence compound of a 25 mole percent Mo composition ($6LaO_{1.5}$-$2MoO_x$). There was also evidence of a small amount of La_2MoO_5, in which Mo has a valence of IV. This diffraction pattern, did not contain any evidence of the Mo^{VI} compounds $La_{10}Mo_2O_{21}$, La_4MoO_9 or $La_6Mo_2O_{15}$ that were observed at higher oxygen partial pressures for a similar ratio of La to Mo. This is interpreted as evidence that the Mo^{VI} compounds containing greater than 15% Mo are not stable at oxygen partial pressures below $2x10^{-6}$ Pa.

Sample LAMO_10, with a composition of 2:1 La:Mo, was found to contain mostly $La_{12}Mo_6O_{35}$. This formula has a mixed molybdenum valence with one Mo^{IV} to five Mo^{VI}. This high average valence of molybdenum is consistent with the fact that the compound becomes stable close to the oxygen partial pressure region where the Mo^{VI} compounds are stable. The x-ray diffraction pattern for this sample is shown in Figure 4.3. Evidence of traces of the mixed valence compounds $La_6Mo_2O_{14}$, which has one Mo^{IV} to one Mo^{VI}, and $La_5Mo_3O_{16}$, which has one Mo^{IV} to five Mo^{VI}, were also seen in the pattern. The primary phase was again the 2:1 compound $La_{12}Mo_6O_{35}$ (one Mo^{IV} to five Mo^{VI}), which was accompanied by minor phases $La_5Mo_3O_{16}$ (one Mo^{IV} to five Mo^{VI}), and $La_5Mo_4O_{16}$ (seven Mo^{IV} to one Mo^{VI}).

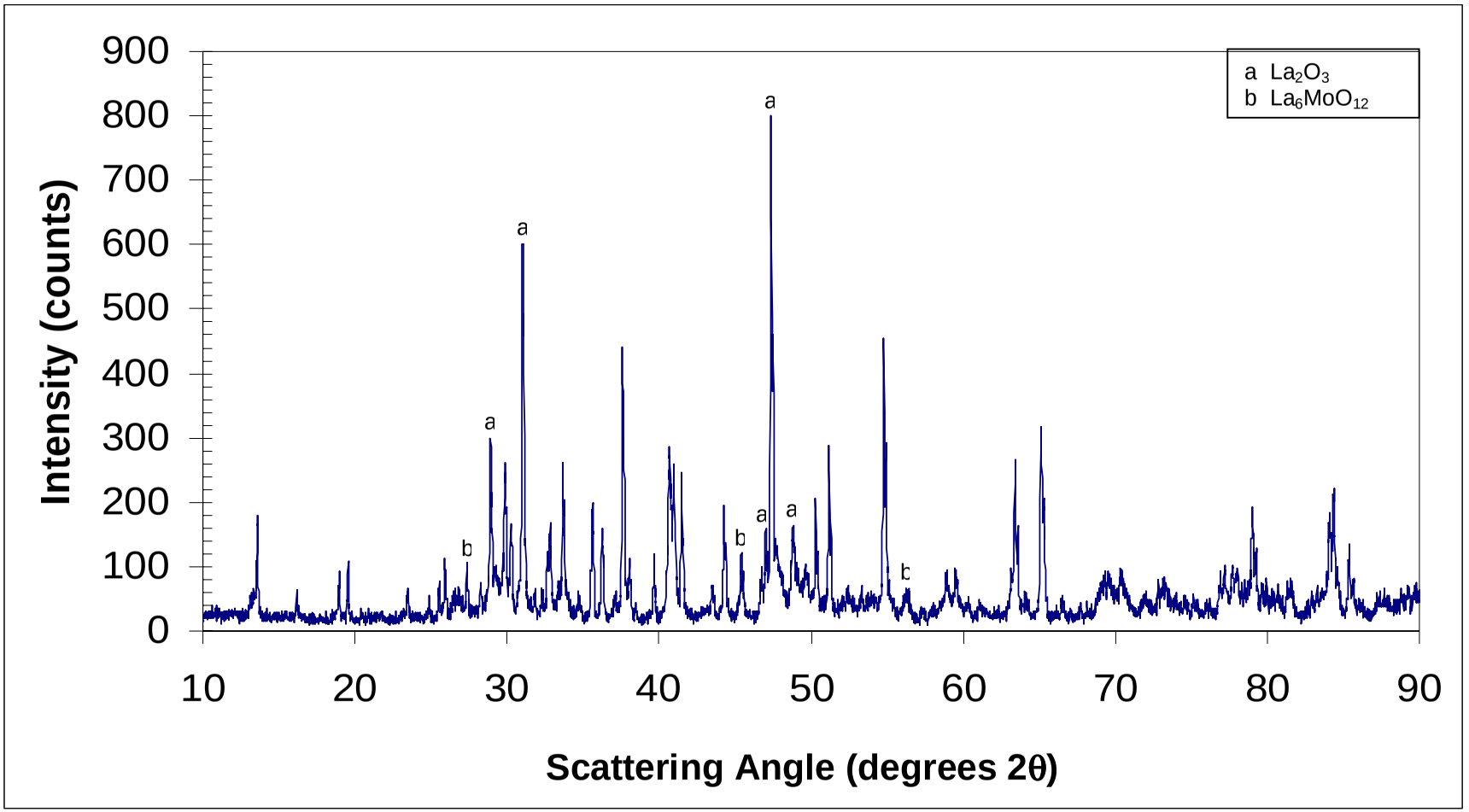

Figure 4.2 XRD Pattern for LAMO_53

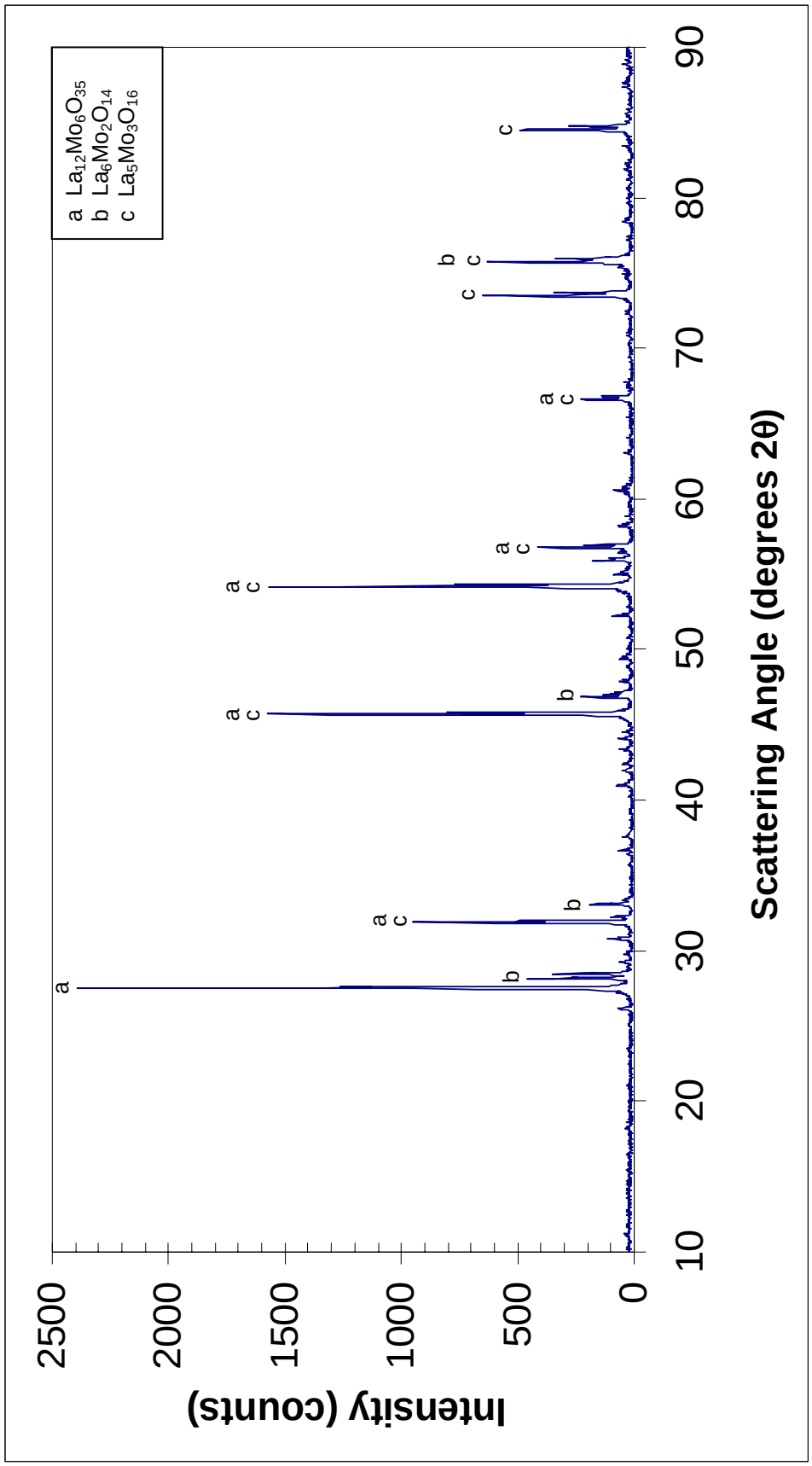

Figure 4.3 XRD pattern for LAMO_10

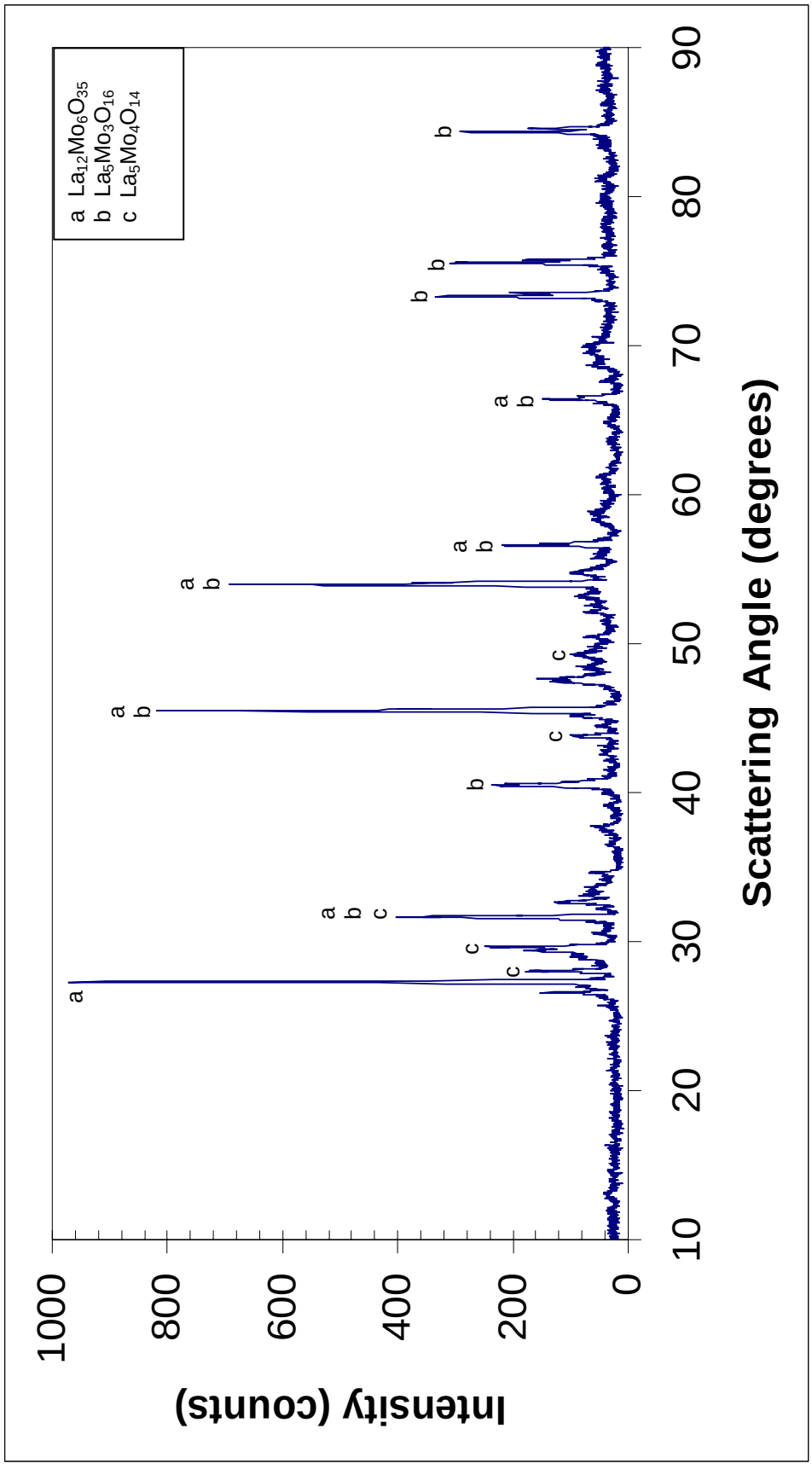

Figure 4.4 XRD Pattern for LAMO_54

Oxygen Partial Pressure of 3x10-7 to 1x10-7 Pa

Several mixed-molybdenum valence compounds were stable in this pressure range. Sample LAMO_60 was prepared from a 3:1 molar ratio and run at an O_2 partial pressure of $2x10^{-7}$ Pa. Examination of the x-ray diffraction pattern, shown in Figure 4.5, confirms the presence of $La_6Mo_2O_{14}$ as the predominant phase. At this lower oxygen partial pressure, the molybdenum valence has reduced to 50% Mo^{IV} and 50% Mo^{VI}. Other minor phases, $La_{10}Mo_4O_{24}$, and $La_4Mo_2O_{11}$ can also be seen in the diffraction pattern, but they may be non-equilibrium phases and are not necessarily stable here. The compound $La_{10}Mo_4O_{24}$ is a suggested phase that has not been previously identified in the literature, and the designation of this formula to the diffraction pattern will be discussed in a later section.

$La_4Mo_2O_{11}$, with a 1:1 Mo^{IV} :Mo^{VI} valence ratio is observed as the only phase present in sample LAMO_61, which was composed of a 2:1 molar ratio and run at the same oxygen partial pressure as LAMO_60. The x-ray diffraction pattern for LAMO_61 is seen in Figure 4.6 and corresponded exactly with the pattern for $La_4Mo_2O_{11}$ that was reported by Gall and Gougeon.[29]

Samples LAMO_10 (2:1 La:Mo, $4.6x10^{-7}$ Pa) and LAMO_34 (2:1 La:Mo, $8.1x10^{-8}$ Pa) were not found to contain any $La_4Mo_2O_{11}$, so the upper and lower stability limits for this compound are defined as $3x10^{-7}$ Pa and $1x10^{-7}$ Pa.

At a molar ratio of 1:1.5 La:Mo and oxygen partial pressure of $2x10^{-7}$ Pa, sample LAMO_62, a compound was formed that could not be identified. The compound's x-ray diffraction pattern, shown in Figure 4.7, could not be matched to any pattern in the Powder Diffraction File database. This compound would be expected to have a Mo

valence less than VI because of the reducing atmosphere, but no compounds were reported in the literature with a La:Mo ratio of 1:1.5 and a Mo valence less than VI. LAMO_62 forms in the same pressure range as mixed-molybdenum valence compounds such as $La_4Mo_2O_{11}$ that have equal parts Mo^{IV} and Mo^{VI} valences; however, the high Mo concentration makes MoO_3 (Mo^{VI} valence) less stable than MoO_2 (Mo^{IV} valence), as previously noted. Therefore, based upon the formulated composition and O_2 partial pressure, the projected formula for this phase is $La_2Mo_3O_{10}$, with a proposed Mo^{IV} to Mo^{VI} valence ratio of 2:1.

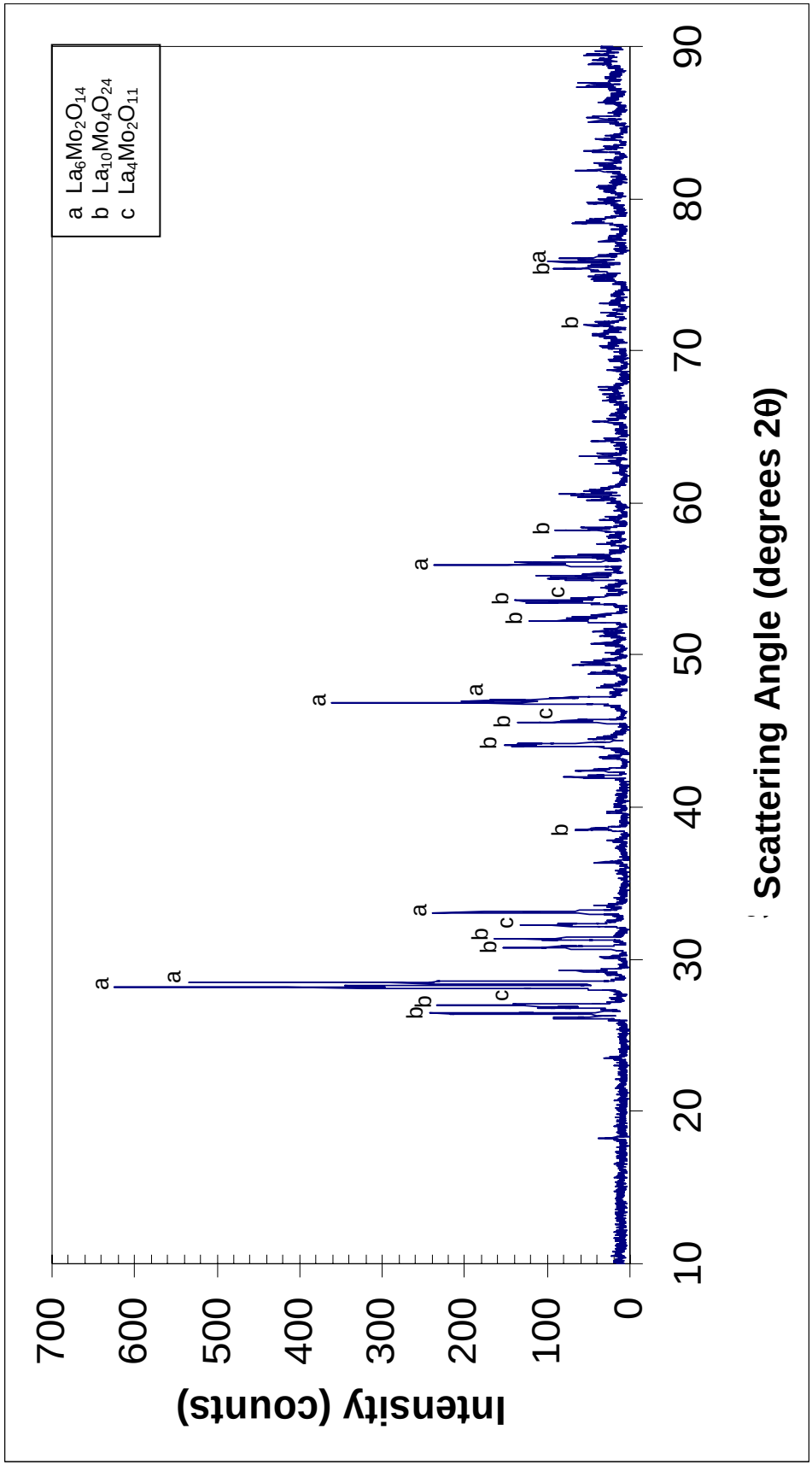

Figure 4.5 XRD Pattern for LAMO_60

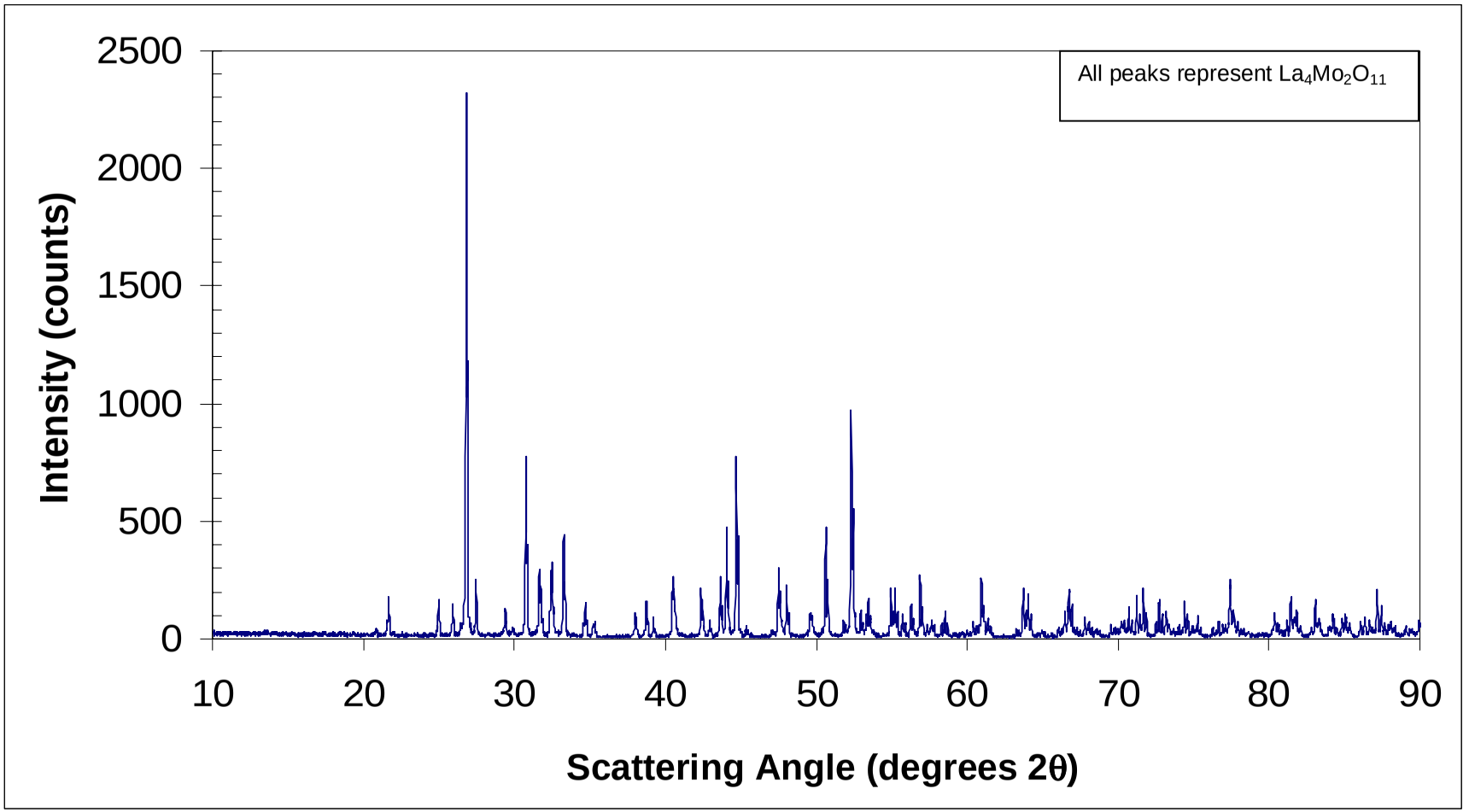

Figure 4.6 XRD Pattern for LAMO_61

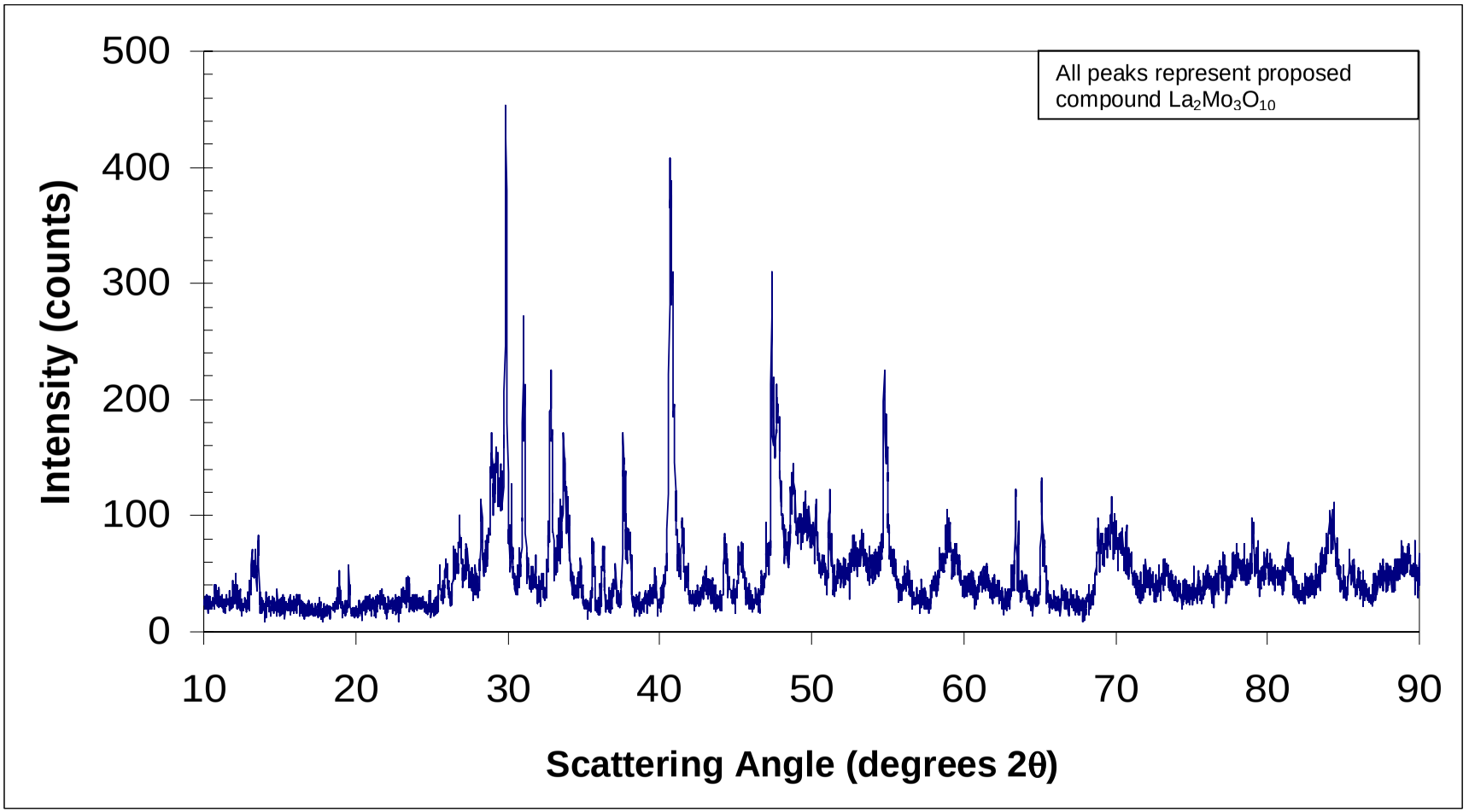

Figure 4.7 XRD Pattern for LAMO_62

Oxygen Partial Pressure of 1x10-7 to 8x10-9 Pa

In this pressure range, the Mo valence of IV forms more readily. At a composition of 6:1 La:Mo, and partial pressure of 8.147×10^{-8} Pa, sample LAMO_57 showed formation of $La_6Mo_2O_{14}$ as the primary compound. Since $La_6Mo_2O_{14}$ is constituted of a 3:1 molar ratio, there was also some La_2O_3 present as expected. A small amount of the Mo^{IV} compound, La_2MoO_5 was also identified.

A similarly high concentration of $La_6Mo_2O_{14}$ was found in sample LAMO_35, which was equilibrated at a much lower partial pressure of 9.7×10^{-9} Pa. For this reason, the lower stability limit for the mixed valence compound $La_6Mo_2O_{14}$ was set at 8×10^{-9} Pa in this composition range. The x-ray diffraction plot for LAMO_35, seen in Figure 4.8, also shows some La_2O_3 peaks and La_2MoO_5 peaks. Due to the high La:Mo (6:1) ratio of samples LAMO_57 and LAMO_35, La_2MoO_5 (2:1 La:Mo) is not considered to be an equilibrium phase here, but simply present because the reaction may not have gone to completion. Furthermore, La_2MoO_5 has a Mo valence of IV, which might require a lower O_2 partial pressure for stability, especially considering that these compositions lie in the La rich portion of the phase diagram, where the Mo^{VI} valence tends to be more stable.

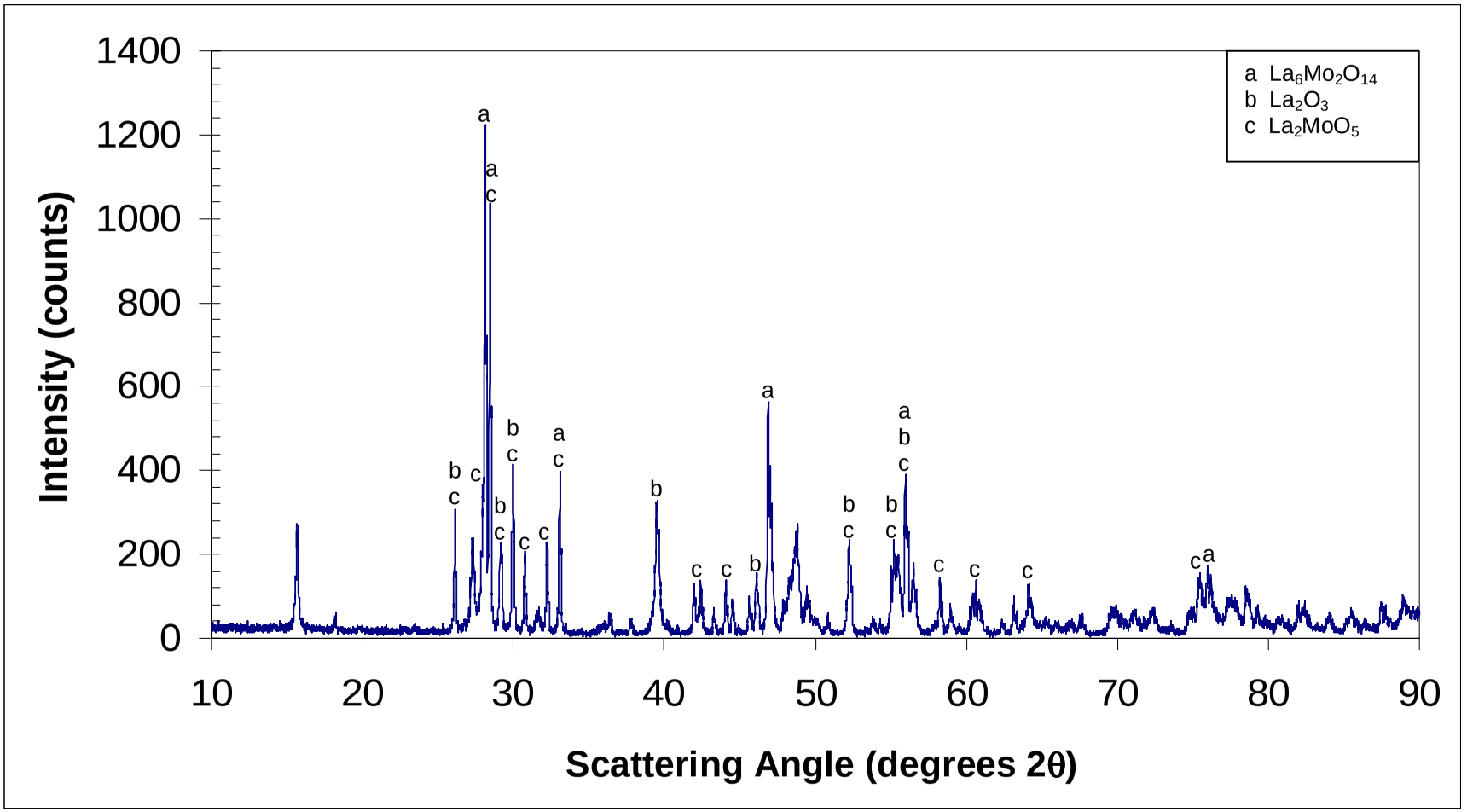

Figure 4.8 XRD Pattern for LAMO_35

At a 2:1 La:Mo ratio, sample LAMO_34 was run at a partial pressure of 8.147×10^{-8} Pa. Its x-ray diffraction pattern corresponds exactly with a pattern previously identified as β-La_2MoO_5 which was believed to be a high temperature Mo^{IV} phase that is stable at very low oxygen partial pressures (2×10^{-9} Pa).[39] This early identification was based on stoichiometry and the assumption that a single-phase sample had been produced. More careful analysis of the diffraction data, seen in Figure 4.9, reveals the presence of $La_2Mo_3O_{10}$ peaks (as designated in Figure 4.7) which suggests this diffraction pattern is multi-phase.

Sample LAMO_32, run at a lower oxygen partial pressure of 9.7×10^{-9} Pa, has a very similar pattern, bearing the same peaks as the major phase with a small amount of the $La_2Mo_3O_{10}$ phase. In an effort to define a new formula for this major phase, the literature was searched for rare-earth molybdates of molar ratios similar to 2:1 with a molybdenum valence less than VI. Torardi, *et al*., published x-ray diffraction patterns for mixed molybdenum valence compounds of a 2.5:1 molar ratio, $Y_5Mo_2O_{12}$ and $Gd_5Mo_2O_{12}$.[31] These patterns were very similar to each other, despite the distance between Y and Gd on the periodic table. Therefore, it was anticipated that if a lanthanum compound of the form $Ln_5Mo_2O_{12}$ exists, it would also have a similar diffraction pattern to $Y_5Mo_2O_{12}$ and $Gd_5Mo_2O_{12}$.

Figure 4.10 depicts the x-ray diffraction pattern for sample LAMO_34 plotted with the pattern for $Y_5Mo_2O_{12}$. Due to similarities between the patterns, it is suggested that the phase formerly designated as β-La_2MoO_5 is actually $La_5Mo_2O_{12}$. The molybdenum valence of such a compound would likely be 3 Mo^{IV} for every Mo^{VI}, so the compound will be identified as $La_{10}Mo_4O_{24}$. Its low average valence of 4.5 is in

accordance with the previously noted stability of this phase at a low oxygen partial pressure.

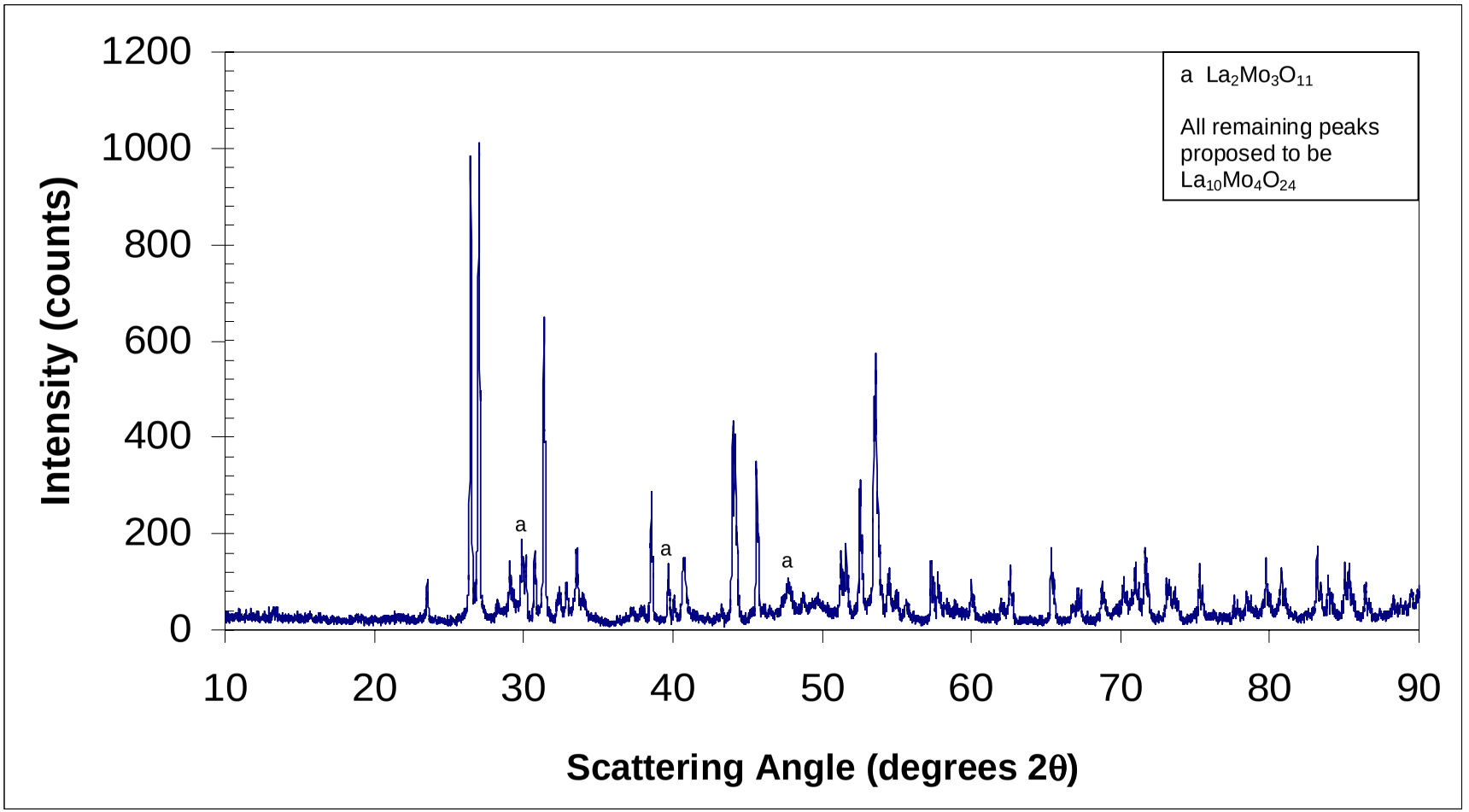

Figure 4.9 XRD Pattern for LAMO_34

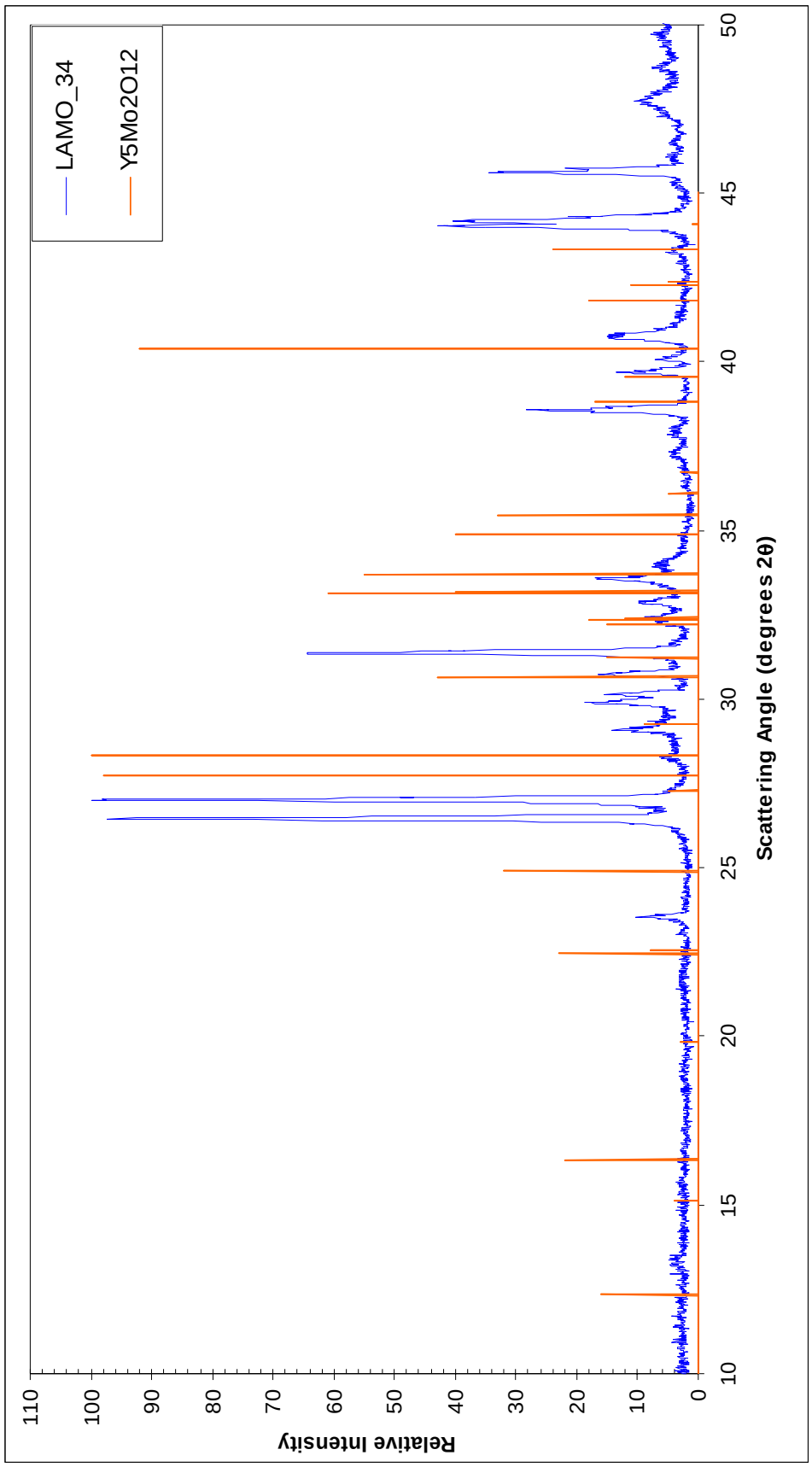

Figure 4.10 XRD Pattern for LAMO_34 with Powder Diffraction File for $Y_5Mo_2O_{12}$

At this same partial pressure with a concentration of approximately 43% Mo, sample LAMO_36 was run. This diffraction pattern displays strong $La_{10}Mo_4O_{24}$ peaks, as well as several secondary peaks that correlate with sample LAMO_62 and are attributed to $La_2Mo_3O_{10}$. At a slightly higher molybdenum concentration, and in a more oxidizing atmosphere, LAMO_58 was processed. The diffraction pattern for this sample matches almost exactly with that of LAMO_36, displaying $La_{10}Mo_4O_{24}$ as the primary phase with the smaller $La_2Mo_3O_{10}$ peaks.

More experiments were run in this region at a molar ratio of 1:1.5 La:Mo to attempt to define the limits of stability for the compound identified as $La_2Mo_3O_{10}$. Sample LAMO_59, was run at 8.147×10^{-8} Pa, and its diffraction pattern shows an excellent match with the pattern for LAMO_62.

At an oxygen partial pressure of 1.6×10^{-8} Pa, sample LAMO_66 was also run at a 1:1.5 molar ratio of La:Mo. The diffraction pattern for this sample, seen in Figure 4.11, reveals mostly molybdenum. $La_2Mo_3O_{10}$ peaks are also present, indicating that this compound is still stable at O_2 partial pressures this low. The remainder of the sample appears to be a small amount of the $La_{10}Mo_4O_{24}$ compound established by LAMO_34. A similar distribution of phases was seen in sample LAMO_64, for the same composition but a still lower partial pressure of oxygen; 9.7×10^{-9} Pa. LAMO_64 shows slightly smaller diffraction peaks for $La_2Mo_3O_{10}$, indicating that this pressure is likely near the lower stability limit for the compound.

Samples LAMO_67 and LAMO_65 contained a 1:2 molar ratio of La:Mo, and were run at oxygen partial pressures of 1.6×10^{-8} and 9.7×10^{-9} Pa, respectively. Due to the higher molybdenum concentration, no evidence of the 2:1 compound referred to as

$La_{10}Mo_4O_{24}$ is noted in either diffraction pattern, and molybdenum is unquestionably the dominant phase. XRD also shows that $La_2Mo_3O_{11}$ is present in a very small amount.

Samples were also prepared in this pressure range at very high molybdenum concentrations (1:4.5). X-ray diffraction data for all of these samples show molybdenum as the primary phase. LAMO_31B was processed at a partial pressure of 9.697×10^{-9} Pa, and its x-ray diffraction pattern is shown in Figure 4.12. This pattern indicates almost 100% molybdenum, with the exception of small peaks that match the pattern for $La_2Mo_3O_{10}$.

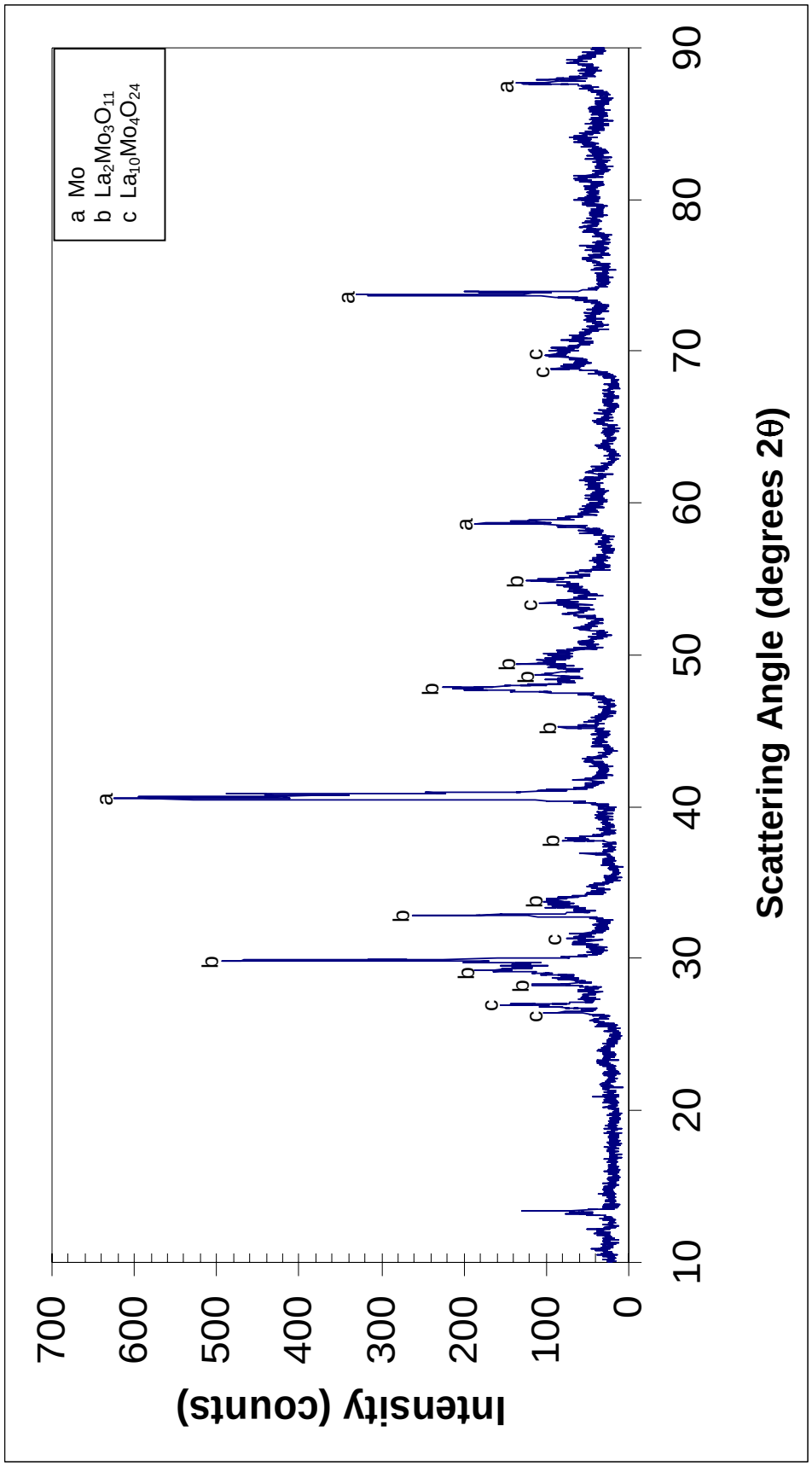

Figure 4.11 XRD Pattern for LAMO_66

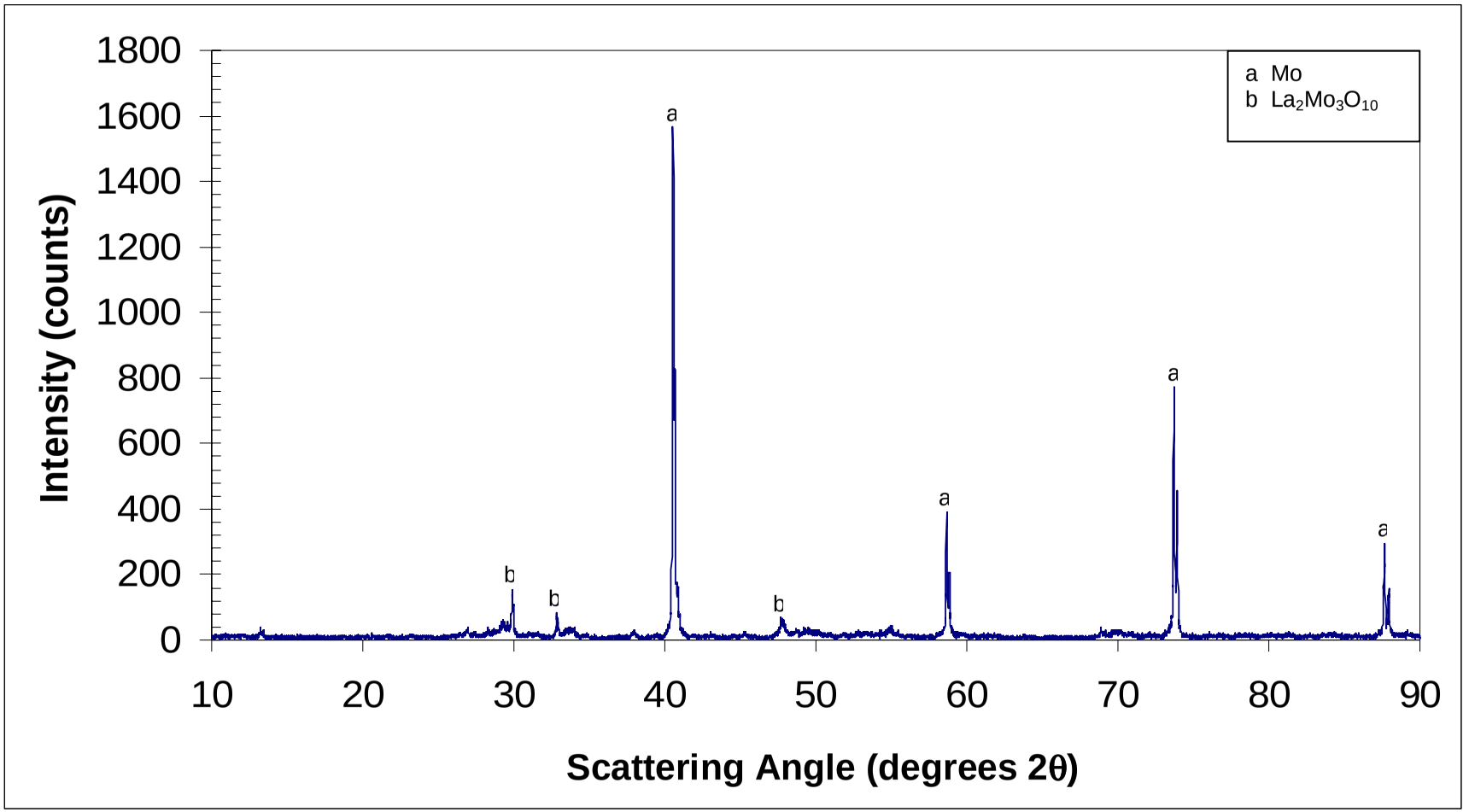

Figure 4.12 XRD Pattern for LAMO_31B

Oxygen Partial Pressure below 8x10-9 Pa

At the 33.33% Mo composition, two samples were produced at very low oxygen partial pressures. The x-ray diffraction pattern for LAMO_20, prepared at 2.168×10^{-9} Pa of oxygen, is seen in Figure 4.13. The primary phase closely correlates with the pattern described as $La_{10}Mo_4O_{24}$ and the diffraction pattern also shows a small amount of Mo. Seeing that this sample contained a 2:1 ratio of La:Mo, the presence of metallic molybdenum further supports the designation of the major phase as a 2.5:1 La:Mo compound, $La_{10}Mo_4O_{24}$.

LAMO_02B was run at the same composition with an oxygen partial pressure of 2.2×10^{-10} Pa, and no reaction occurred at all, yielding the unreacted starting materials, La_2O_3 and molybdenum. For this reason, the lower limit of the region in which $La_{10}Mo_4O_{24}$ is stable is estimated as 1×10^{-9} Pa. This line was extended across the phase diagram, to indicate that no lanthanum molybdates are expected to form at partial pressures below approximately 1×10^{-9} Pa.

LAMO_30 was made up of 81.82% molar molybdenum, and processed at a partial pressure of 2.2×10^{-9}. The XRD pattern derived from the product, displayed in Figure 4.14, was compared to the pattern for LAMO_31B which was also 81.82% Mo, but processed at 9.697×10^{-9} Pa. The diffraction data for LAMO_30 displays the presence of $La_{10}Mo_4O_{24}$ in approximately the same intensity as $La_2Mo_3O_{10}$ occurred in LAMO_31. The formation of $La_{10}Mo_4O_{24}$ (3 Mo^{IV} to 1 Mo^{VI}) rather than $La_2Mo_3O_{11}$ (2 Mo^{IV} to 1 Mo^{VI}) is an indication that $La_2Mo_3O_{10}$ is not stable at such low partial pressures of oxygen, so its lower stability limit is estimated at approximately 8×10^{-9} Pa.

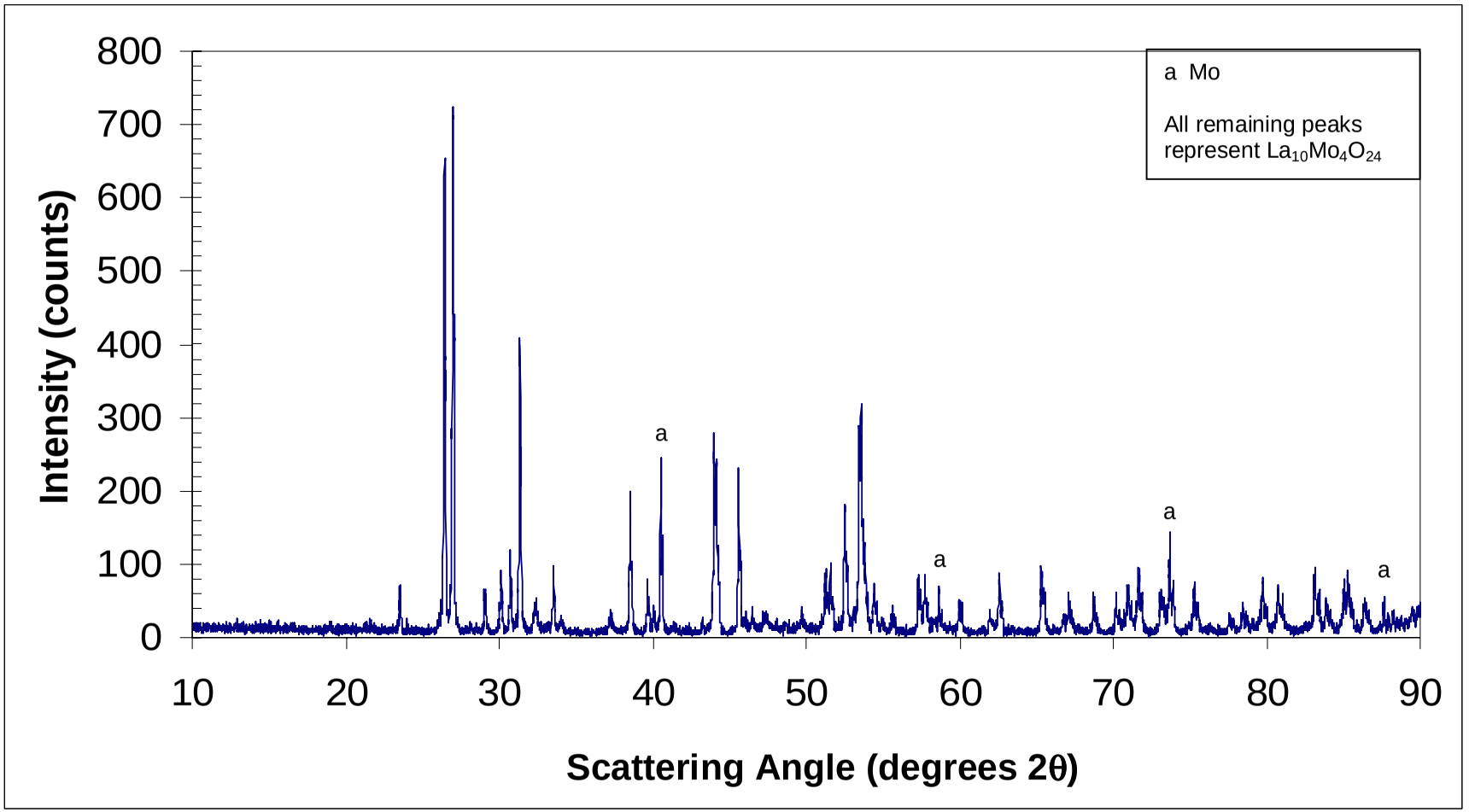

Figure 4.13 XRD Pattern for LAMO_20

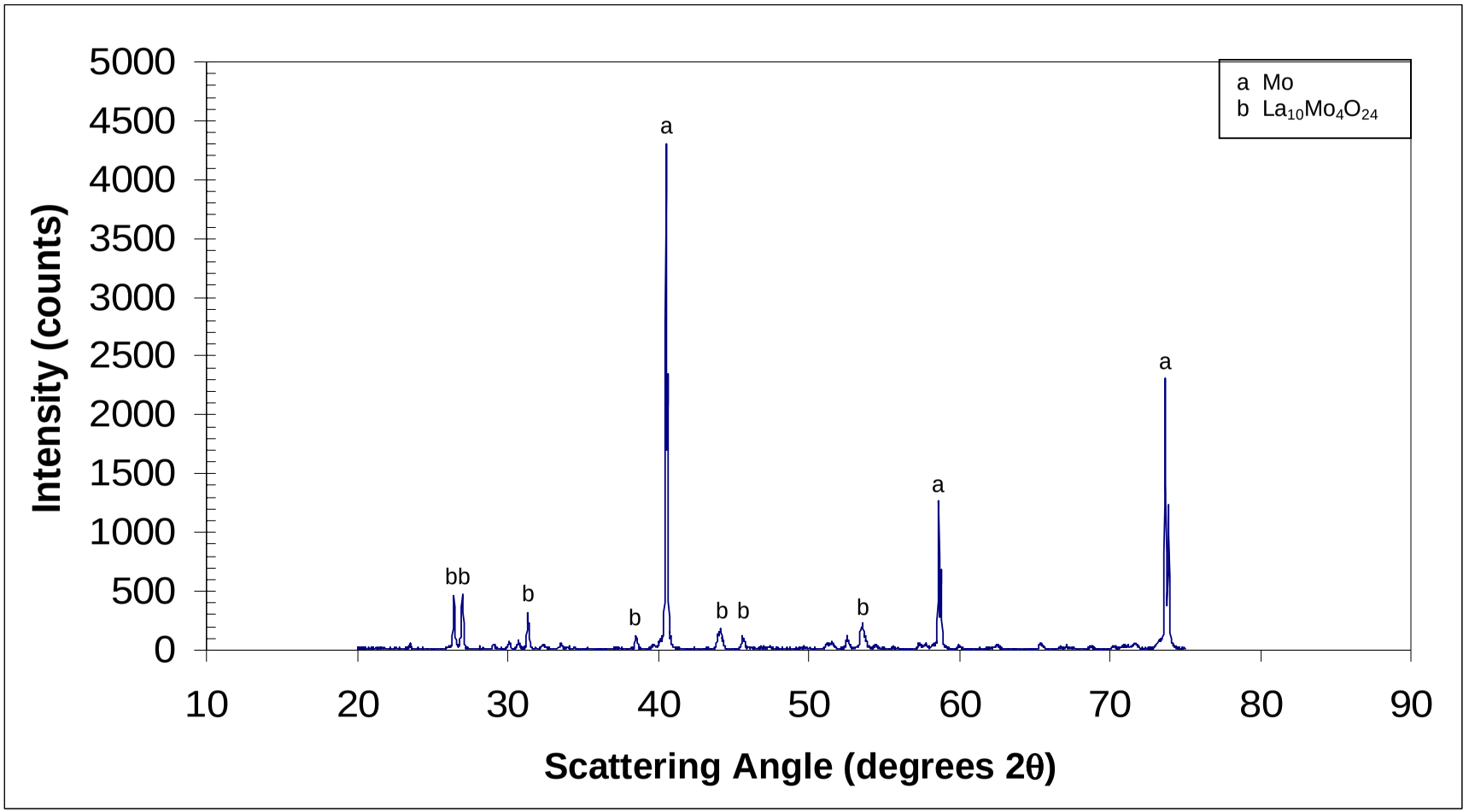

Figure 4.14 XRD Pattern for LAMO_30

The $LaO_{1.5}$-MoO_x system at 1000ºC

The isothermal phase diagram for the $LaO_{1.5}$-MoO_x system at 1000ºC is seen in Figure 4.15. Previous work in this system confirmed the formation of La_2MoO_6, and $La_4Mo_2O_{11}$ at a 2:1 La:Mo ratio, and they are positioned at the appropriate O_2 partial pressures on the diagram.[39] The phase identified in this study as $La_{10}Mo_4O_{24}$ was also reported in the earlier work at a 2:1 molar composition, but it is positioned on this phase diagram at the appropriate La:Mo ratio of 2.5:1. Points plotted on the phase diagram represent the experiments run in this study, which emphasized the equilibria at low partial pressures of oxygen. Using x-ray diffraction, the resulting compounds were identified, and are presented in Table 4.2 along with the molar compositions and oxygen partial pressures of formation.

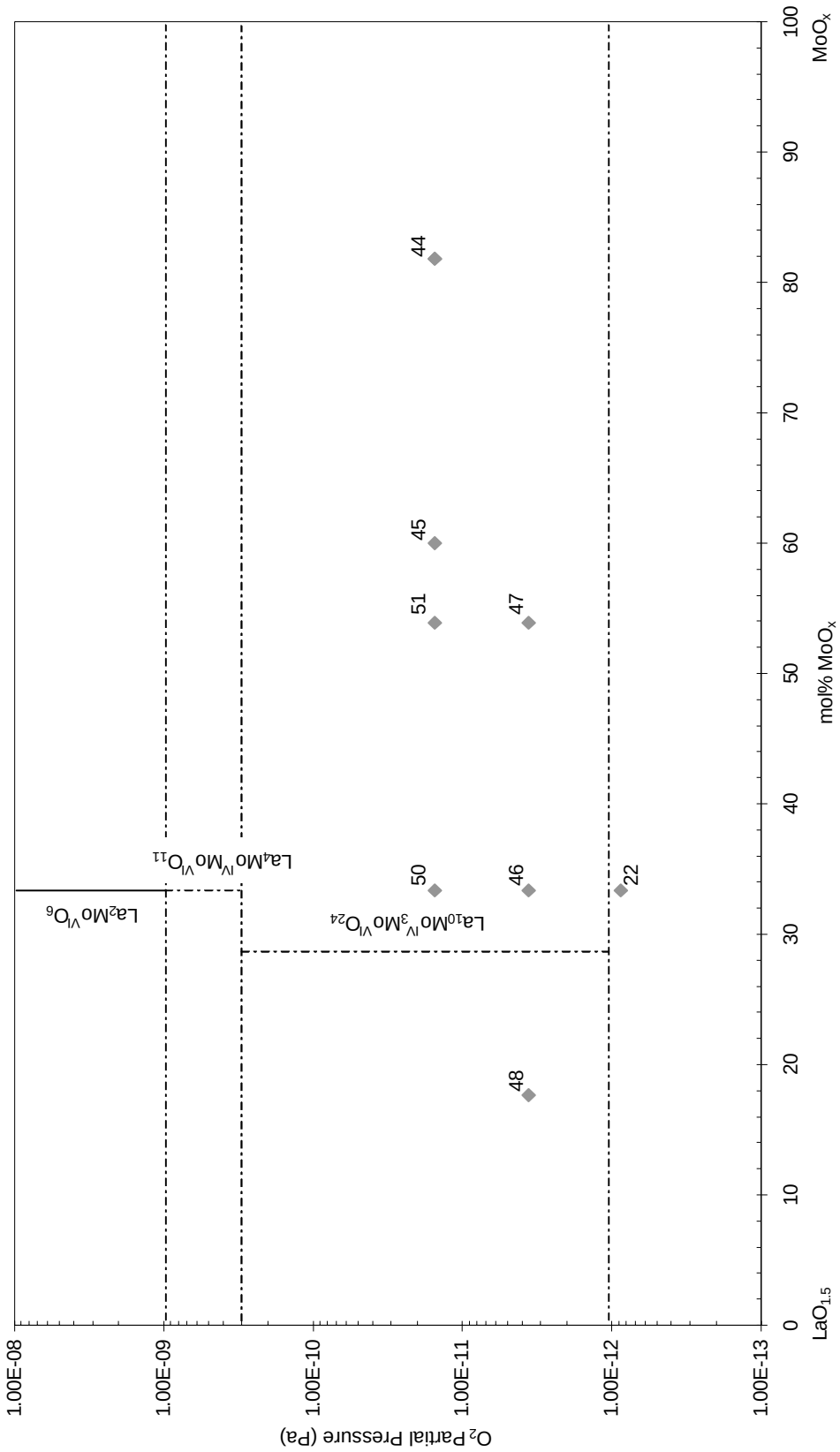

Figure 4.15 Phase equilibria in the $LaO_{1.5}$-MoO_x system at 1000ºC

Table 4.2 Phases resulting from experiments with La_2O_3 and Mo at 1000°C

Sample Name	La:Mo Ratio	Molar % Mo	O_2 Partial Pressure (Pa)	Process Time (hours)	Phases Present
LAMO_50	2:1	33.33	1.530E-11	84	**$La_{10}Mo_4O_{24}$,** La_2O_3, Mo_2C
LAMO_51	1:1.17	53.92	1.530E-11	84	**Mo_2C,** $La_{10}Mo_4O_{24}$
LAMO_45	1:1.5	60.00	1.530E-11	72	**Mo_2C,** $La_{10}Mo_4O_{24}$
LAMO_44	1:4.5	81.82	1.530E-11	72	**Mo_2C,** $La_{10}Mo_4O_{24}$
LAMO_49	1:4.5	81.82	1.530E-11	84	**Mo_2C,** $La_{10}Mo_4O_{24}$
LAMO_48	4.67:1	17.64	3.612E-12	60	**La_2O_3,** $La_{10}Mo_4O_{24}$
LAMO_46	2:1	33.33	3.612E-12	96	**$La_{10}Mo_4O_{24}$,** La_2O_3, Mo_2C
LAMO_47	1:1.17	53.92	3.612E-12	60	**Mo_2C,** $La_{10}Mo_4O_{24}$
LAMO_22	2:1	33.33	8.744E-13	48	**La_2O_3,** Mo, $La_{10}Mo_4O_{24}$

Two of the samples run at a 2:1 molar ratio of La:Mo formed $La_{10}Mo_4O_{24}$ as the primary phase, namely LAMO_46 and LAMO_50 prepared at $3.61x10^{-12}$ and $1.53x10^{-12}$ Pa O_2, respectively. This x-ray diffraction pattern reveals that most of the stating powders did not react, and that only a small amount of $La_{10}Mo_4O_{24}$ formed. The lower stability limit of this phase was therefore estimated as $1x10^{-12}$ Pa on the phase diagram.

One major problem that became apparent during these experiments hindered further analysis of phase equilibria in this system at 1000ºC. All of the samples run at oxygen partial pressures between $1.53x10^{-11}$ Pa to $3.612x10^{-12}$ Pa formed significant amounts of Mo_2C, which was clearly evident in their x-ray diffraction patterns. At partial pressures in this range at 1000ºC, the reaction of molybdenum with carbon is apparently much more likely than a reaction with La_2O_3. The only way to avoid the formation of Mo_2C at this temperature and pressure is to replace CO_2 with another gas mixture that can be used in a similar manner to control the atmosphere in the furnace

tube. N_2O was considered, but cannot be used because it is easily combustible and poses risk of explosion in a sealed furnace at such high temperatures.

The $YO_{1.5}$-MoO_x system at 1200ºC

Experiments in the $YO_{1.5}$-MoO_x system at 1200ºC evaluated 2:1 molar compounds similar to those formed in the $LaO_{1.5}$-MoO_x system. Attempts were made to produce compounds of varying molybdenum valences by experimenting over a range of pressures. Samples processed with Y_2O_3 and Mo have not yielded enough conclusive data to produce a preliminary phase diagram. Table 4.3 shows the molar ratios and experimental conditions for these samples.

Table 4.3 Phases resulting from experiments with Y_2O_3 and Mo at 1200°C

Sample Name	Y:Mo Ratio	Molar % Mo	O_2 Partial Pressure (Pa)	Process Time (hours)	Phases Present
YMO_05	2:1	33.33	2.168E-09	24	**Y_2MoO_5,** $Y_5Mo_2O_{12}$, MoO_2, Y_2O_3, Y_6MoO_{12}
YMO_03	2:1	33.33	2.168E-09	50	**Y_6MoO_{12},** Y_2O_3, Mo
YMO_13	1:4.5	81.82	2.168E-09	50	**Mo,** Y_2O_3
YMO_01	2:1	33.33	1.956E-11	50	**Y_2O_3,** Mo

Sample YMO_05 was processed with a 2:1 ratio of Y:Mo at $2.2x10^{-9}$ Pa of O_2. The major phase present is Y_5MoO_{12}, which is the only mixed-molybdenum valence yttrium molybdate reported in the literature. In this case, Y_5MoO_{12} may not be a stable equilibrium phase because sample YMO_05 was only heated for 24 hours and the reaction may not have reached equilibrium. For this reason, YMO_03, which uses the same composition and partial pressure, is a more reliable basis for verifying stable phases

because it ran for 50 hours. The x-ray diffraction pattern for sample YMO_03, which is seen in Figure 4.16, reveals Y_6MoO_{12} as a stable phase at this temperature and oxygen partial pressure. This compound displays a molybdenum valence of VI, as in the equivalent lanthanum molybdate, but remains stable at lower oxygen partial pressures than La_6MoO_{12}. Diffraction data shows that Y_6MoO_{12} peaks appear at the same scattering angles as many of the Y_2O_3 peaks, which makes those compounds difficult to differentiate. It was noted when using the PC Identify program to compare YMO_03 with the PDF for Y_2O_3 that some peaks had an unusually high intensity. These very high peaks are the ones that overlap with the Y_6MoO_{12} pattern, so it can be assumed that for those peaks, both phases are contributing to the peak intensity. Mo was the primary phase, which is reasonable since this sample represented a 2:1 ratio, and presence of Y_6MoO_{12} (6:1) would leave substantial metallic Mo un-reacted. The mixed-valence compound Y_5MoO_{12} was not observed in any sample except YMO_05 and may not be stable at this temperature.

Using a more reducing atmosphere, sample YMO_01 was run at an oxygen partial pressure of 1.956x10-11 Pa. If mixed molybdenum valence compounds exist in the $YO_{1.5}$-MoO_x system at 1200ºC, they would be expected to exist in this region. The diffraction data for YMO_01 show only Y_2O_3 and Mo peaks, indicating that the powders did not react to form any yttrium molybdates. This is in accordance with the literature, which have not reported any mixed molybdenum valence compounds with Y_2O_3 and Mo. Sample YMO_13 was run using 81.82% Mo at the partial pressure where the Mo^{VI} compound, Y_6MoO_{12}, was stable, but no evidence of molybdate formation was noted.

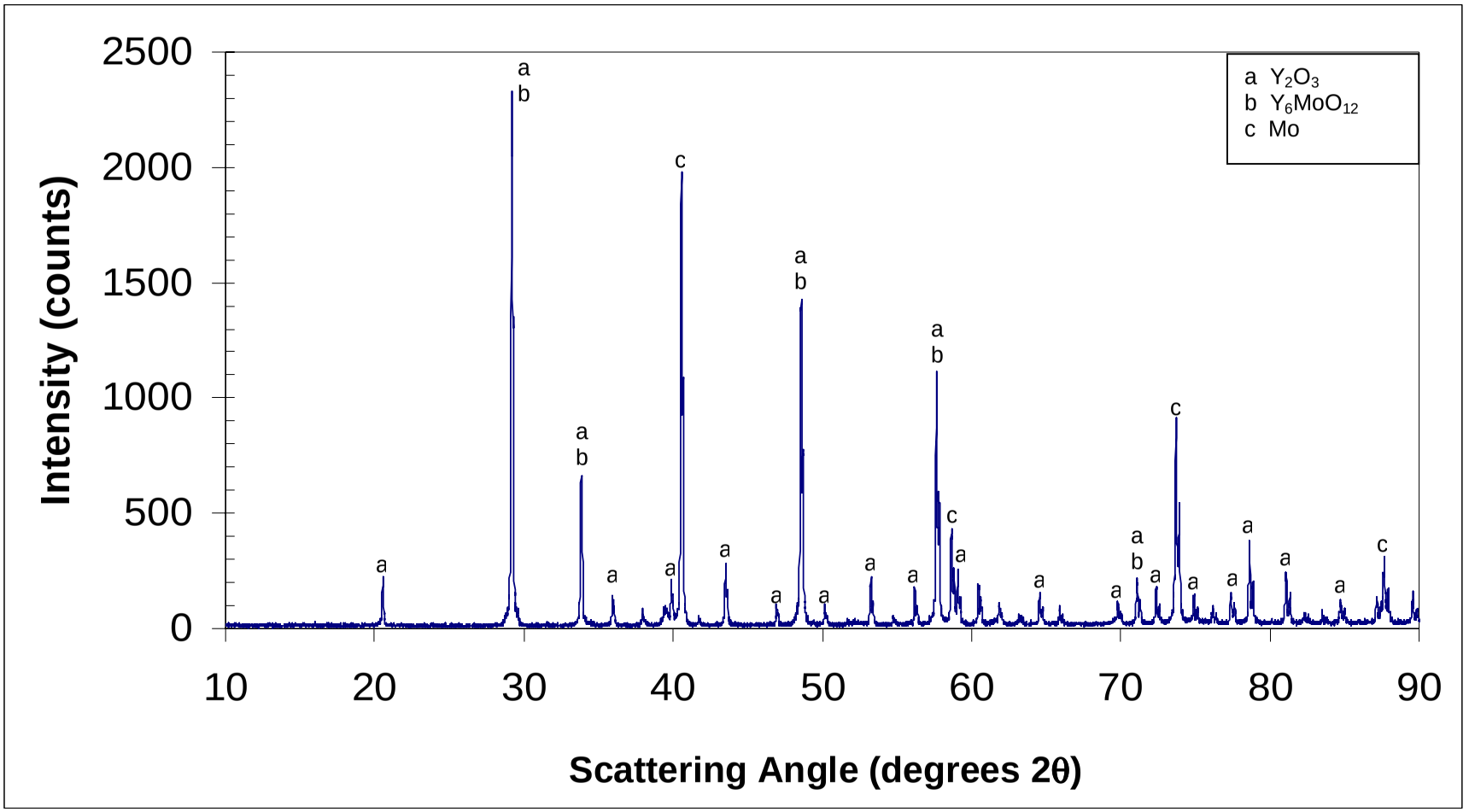

Figure 4.16 XRD Pattern for Sample YMO_03

The $YO_{1.5}$-MoO_x system at 1000ºC

Experiments at 1000ºC were run over a range of oxygen partial pressures from $2.645x10^{-6}$ to $3.612x10^{-12}$ Pa. The experimental conditions and the results from the phase identification are seen in Table 4.4.

Table 4.4 Phases resulting from experiments with Y_2O_3 and Mo at 1000°C

Sample Name	Y:Mo Ratio	Molar % Mo	O_2 Partial Pressure (Pa)	Process Time (hours)	Phases Present
YMO_06	2:1	33.33	2.645E-06	72	**$Y_5Mo_2O_{12}$,** Y_2O_3
YMO_12	2:1	33.33	4.641E-07	48	**Y_2O_3,** Y_6MoO_{12}, $Y_5Mo_2O_{12}$
YMO_09	2:1	33.33	8.147E-08	72	**Y_6MoO_{12},** Y_2O_3, $Y_5Mo_2O_{12}$
YMO_20	2:1	33.33	1.530E-11	70	**Y_2O_3,** Mo_2C, $Y_5Mo_2O_{12}$
YMO_21	1:1.5	60.00	1.530E-11	70	**Mo_2C,** Y_2O_3, $Y_5Mo_2O_{12}$
YMO_19	6:1	14.29	3.612E-12	72	**Y_2O_3,** Mo_2C
YMO_18	4.06:1	19.76	3.612E-12	72	**Y_2O_3,** Mo_2C
YMO_17	2:1	33.33	3.612E-12	72	**Y_2O_3,** Mo_2C

At the 2:1 molar ratio of Y:Mo, Y_6MoO_{12} was found to be stable in samples YMO_12 and YMO_09. Being a Mo^{VI} compound, it would also be expected to form at a higher oxygen partial pressure, as in sample YMO_06. Instead, the only yttrium molybdate that forms in this sample is $Y_5Mo_2O_{12}$. This may indicate that $Y_5Mo_2O_{12}$ formed in this sample as an intermediate before the reaction reached equilibrium, and formed Y_6MoO_{12}. Therefore, the possibility of a mixed molybdenum valence compound has been observed in the $YO_{1.5}$-MoO_x system; however its stability limits have not been defined.

All of the experiments that were run at low partial pressures of oxygen formed Mo_2C, as with the La_2O_3-Mo experiments at 1000°C. Because of this reaction of molybdenum with carbon dioxide, phase equilibria could not be analyzed at or below an oxygen partial pressure of $1.53x10^{-11}$ Pa.

The ZrO_2-MoO_x system

Preliminary experiments involving ZrO_2 and Mo were performed at 1200°C and 1000°C. The results of these experiments, shown in Table 4.5, show that no zirconium molybdates were formed. Based on the oxygen partial pressures that yield stable compounds for the $LaO_{1.5}$-MoO_x system, experiments at 1200°C were run at an O_2 partial pressure of $4.6x10^{-7}$ Pa and $2x10^{-7}$ Pa, and experiments at 1000°C at an O_2 partial pressure of $1.53x10^{-11}$ Pa. By comparing samples ZRMO_01 with ZRMO_03 (both composed of equimolar ZrO_2 and Mo), it is apparent that MoO_2 is stable in sample ZRMO_03, run at $4.641x10^{-7}$ Pa, indicating that this is below the partial pressure of oxygen where Mo^{VI} reduces to Mo^{IV}. If a mixed-valence zirconium molybdate could be formed, it would be expected in this pressure range; however, all of the diffraction patterns show the presence of only ZrO_2, Mo, MoO_2, or Mo_2C across a range of compositions. These diffraction data indicate that no zirconium molybdate is stable at these temperatures, and also did not reveal any evidence of the compound $ZrMo_2O_8$ that was reported in the literature. This compound was reported to form by quenching from 850ºC, but the reaction atmosphere was not specified. The current laboratory apparatus is incapable of quenching samples, so future attempts to synthesize this compound may require a modified furnace. Furthermore, the gas flow mixture would need to be modified due to the formation of Mo_2C below 1000ºC.

Table 4.5 Phases resulting from experiments with ZrO_2 and Mo

Sample Name	Zr:Mo Ratio	Molar % Mo	Temperature (°C)	O_2 Partial Pressure (Pa)	Process Time (hours)	Phases Present
ZRMO_06	1:1	50.00	1000	1.530E-11	70	**ZrO_2,** Mo_2C
ZRMO_07	1:3	75.00	1000	1.530E-11	70	**Mo_2C,** ZrO_2
ZRMO_01	1:1	50.00	1200	1.976E-07	60	**ZrO_2,** Mo
ZRMO_02	2.33:1	30.00	1200	4.641E-07	60	**ZrO_2,** MoO_2
ZRMO_03	1:1	50.00	1200	4.641E-07	60	**ZrO_2,** MoO_2
ZRMO_04	1:2.33	70.00	1200	4.641E-07	60	**MoO_2,** ZrO_2
ZRMO_05	1:9	90.00	1200	4.641E-07	60	**Mo,** ZrO_2, MoO_2

CHAPTER 5

CONCLUSIONS

Seven compounds of varying composition and molybdenum valence were found to be stable in the $LaO_{1.5}$-MoO_x system at 1200°C between O_2 partial pressures of $1x10^{-4}$ Pa and $1x10^{-10}$ Pa. The Mo^{VI} compounds are stable at the highest partial pressures of O_2, with La_2MoO_6 being stable down to $2x10^{-6}$ Pa and La_6MoO_{12} stable as low as $3x10^{-7}$ Pa. Several mixed molybdenum valence compounds were also observed at 1200ºC. The compound $La_6Mo^{IV}Mo^{VI}O_{14}$ was found to be stable between O_2 partial pressures of $3x10^{-7}$ Pa and $8x10^{-9}$ Pa. The compound $La_4Mo^{IV}Mo^{VI}O_{11}$ was determined as stable between $3x10^{-7}$ Pa and $1x10^{-7}$ Pa, while $La_{12}Mo^{IV}Mo^{VI}{}_5O_{35}$ is stable in the O_2 partial pressure stability range of $2x10^{-6}$ Pa to $3x10^{-7}$ Pa.

A previously unreported phase was identified at a 1:1.5 La:Mo molar ratio between the O_2 partial pressures of $3x10^{-7}$ Pa and $8x10^{-9}$ Pa. Based on the partial pressure range in which it exists, this compound is believed to have a mixed molybdenum valence of two Mo^{IV} for one Mo^{VI}, which yields the chemical formula $La_2Mo^{IV}{}_2Mo^{VI}O_{10}$.

Between partial pressures of $1x10^{-7}$ Pa and $1x10^{-9}$ Pa, using a 2:1 molar La:Mo ratio, samples exhibited a phase that was reported by Hill[39] in earlier work as a Mo^{IV} compound, β-La_2MoO_5. X-ray data obtained in this work revealed that these samples were actually multi-phase, containing small amounts of $La_2Mo_3O_{10}$ at higher O_2 partial pressures and Mo at lower O_2 partial pressures. After considering the molar composition, experimental O_2 partial pressures, and comparison with diffraction patterns for $Y_5Mo_2O_{12}$ and $Gd_5Mo_2O_{12}$, the formula $La_{10}Mo^{IV}{}_3Mo^{VI}O_{24}$ is suggested. Stability limits for this phase are O_2 partial pressures from $1x10^{-7}$ Pa to $1x10^{-9}$ Pa.

In the $LaO_{1.5}$-MoO_x system at 1000ºC, $La_{10}Mo_4O_{24}$ was concluded to be stable between partial pressures of $3x10^{-10}$ Pa and $14x10^{-12}$ Pa. It was also discovered that, in a highly reducing atmosphere (O_2 partial pressure less than $1x10^{-10}$ Pa), Mo_2C forms more readily than the rare-earth molybdates. This hindered further definition of the phase equilibria at 1000ºC.

In the $YO_{1.5}$-MoO_x system, the mixed-molybdenum valence compound $Y_5Mo_2O_{12}$ was observed at 1200ºC with O_2 partial pressure of $2.168x10^{-9}$ Pa and at 1000ºC between the partial pressures of $2.645x10^{-6}$ Pa and $1.53x10^{-11}$ Pa. This confirms the existence of this compound, although the stability of the compound at these temperatures remains undefined. Preliminary experiments in the ZrO_2-MoO_x system did not result in the formation of any zirconium molybdates at 1000ºC or 1200ºC.

CHAPTER 6

RECOMMENDATIONS

Several recommendations are being made for future research in the area of phase equilibria for rare-earth oxide and molybdenum oxide systems. Although extensive research has already been performed in the $LaO_{1.5}$-MoO_x system, more experiments are suggested at higher molybdenum concentrations to explore the possible formation of other compounds with a molybdenum valence less than VI. Further investigation should aim to confirm the formulas of the compounds referred to here as $La_{10}Mo_4O_{24}$ and $La_2Mo_3O_{10}$. Experiments should be run using a 2.5:1 La:Mo ratio to attempt to produce a pure sample and diffraction pattern for the phase believed to be $La_{10}Mo_4O_{24}$. Weight change (oxidation) experiments, perhaps using thermogravimetric analysis (TGA), may be helpful in determining molecular formulas of both phases. Also, crystallographic analysis would be effective in confirming the existence and identity of single phase compounds.

In the $YO_{1.5}$-MoO_x system, experiments are needed at varied La:Mo ratios to fully assess the existence of mixed-molybdenum valence compounds formed with Y_2O_3. Efforts should be made to produce a pure sample of $Y_5Mo_2O_{12}$ using the proper molar composition of starting materials to determine its stability in this region. Also, phase equilibria in this system would be better defined if more experiments were run over a broad range of compositions and partial pressures of oxygen, as in the La_2O_3 system. Many of the samples still appeared to contain Y_2O_3, so it is recommended that the samples be heated for longer times to ensure that the reaction has reached equilibrium.

Preliminary work in the ZrO_2-MoO_x system should be extended to a broader range of oxygen partial pressures and temperatures to attempt to synthesize a zirconium molybdate. The experimental setup should be modified to allow for quenching to attempt to synthesize $ZrMo_2O_8$ as reported in the literature. Also, additional systems, such as CeO_2-MoO_x, should be examined experimentally at high temperatures and low O_2 partial pressures to complement the work that has been done in the La system.

Much of the phase equilibria at 1000ºC for the rare-earth oxides with molybdenum remain unclear in this study due to the formation of Mo_2C from CO_2 in the gas flow system. Gas mixture such as Ar-O_2 might be used to control the oxygen partial pressure in the furnace tube at lower temperatures.

Finally, the phenomenon that prompted this research, the ability of these oxides to plastically deform, ought to be studied. Pellets of powder starting materials can be pressed and sintered in the furnace to reproduce pure phases that have been identified in the $LaO_{1.5}$-MoO_x system. Hardness testing can then be performed on the samples, perhaps using nanoindentation. Compounds with various valences of molybdenum should be compared to help clarify the role of molybdenum valence in plastic deformation of rare-earth molybdates. As research progresses in other rare-earth oxide systems, new phases and compounds bearing different valences of molybdenum should be similarly analyzed.

APPENDIX A

The following describes thermodynamic calculations used to determine O_2 partial pressure and gas equilibria in a combined flow of CO_2 and H_2.

O_2 partial pressure can be determined using the equilibrium reaction:

$$H_2 + \frac{1}{2}O_2 \leftrightarrow H_2O$$

According to molar Gibbs Free Energy:

$$\overline{G}_{H_2} + \frac{1}{2}\overline{G}_{O_2} \leftrightarrow \overline{G}_{H_2O}$$

Also, the following can be applied:

$$\overline{G}_A = G_A^\circ + RT \ln p_A$$

$$G_{H_2}^\circ + RT \ln p_{H_2} + \frac{1}{2}G_{O_2}^\circ + \frac{1}{2}RT \ln p_{O_2} = G_{H_2O}^\circ + RT \ln p_{H_2O}$$

Re-arranging the above equations:

$$G_{H_2}^\circ + \frac{1}{2}G_{O_2}^\circ - G_{H_2O}^\circ = -RT \ln\left(\frac{p_{H_2O}}{(p_{H_2})(p_{O_2})^{\frac{1}{2}}}\right)$$

$$\Delta G^\circ = -RT \ln\left(\frac{p_{H_2O}}{(p_{H_2})(p_{O_2})^{\frac{1}{2}}}\right)$$

Defining k_p as:

$$k_p = \frac{p_{H_2O}}{(p_{H_2})(p_{O_2})^{\frac{1}{2}}}$$

For this system,

$$\Delta G^\circ = \Delta H^\circ - T\Delta S^\circ = -247{,}500 + T(55.85) \qquad [J]$$

$$R = 8.3144 \qquad [\frac{J}{K \cdot mol}]$$

Substituting for ΔG^o and R,

$$-247{,}500 + 55.85T = (-8.3144)(T)\ln(k_p)$$

Re-arranging,

$$\ln k_p = \frac{29767.632}{T} - 6.717$$

$$k_p = \exp\left(\frac{29767.632}{T} - 6.717\right)$$

Substituting with the above definition of k_p,

$$\frac{p_{H_2O}}{p_{H_2}} = \left(p_{O_2}\right)^{\frac{1}{2}} \exp\left(\frac{29767.632}{T} - 6.717\right)$$

Thus at 2000K, for an O_2 partial pressure of $1x10^{-11}$ atm:

$$\frac{p_{H_2O}}{p_{H_2}} = 0.01135$$

With an H_2 pressure of 1 atm, the pressure of H_2O must be 0.01135 atm.

The same calculations are also performed for CO_2, using the following equation:

$$CO + \frac{1}{2}O_2 \leftrightarrow CO_2$$

In this system, the Gibbs free energy is defined as:

$$\Delta G^\circ = \Delta H^\circ - T\Delta S^\circ = -282{,}400 + T(86.81) \qquad [J]$$

$$\Delta G^\circ = -RT \ln\left(\frac{p_{CO_2}}{\left(p_{CO}\right)\left(p_{O_2}\right)^{\frac{1}{2}}}\right) = -RT \ln k_p$$

Combining the equations and substituting for R=8.3144 [J/mol*K]:

$$\frac{p_{CO_2}}{p_{CO}} = \left(p_{O_2}\right)^{\frac{1}{2}} \exp\left(\frac{33965.169}{T} - 10.441\right)$$

Thus at 2000K, for an O_2 partial pressure of $1x10^{-11}$ atm:

$$\frac{p_{CO_2}}{p_{CO}} = 0.002193$$

With a CO pressure of 1 atm, the pressure of CO_2 must be 0.002193 atm.

APPENDIX B

The following is the Visual Basic program code used to perform calculations detrmining O_2 partial pressure for 1 atm total pressure from a molar ratio of CO_2 to H_2 gas at a specific temperature.

```
Private Sub CB_Run_Click()
Truetemp# = Val(TB_Temp.text) + 273
Kp# = Exp(-4197.5 / Truetemp# + 3.724)
vala# = 1 – Kp#
valb# = 2 * Kp#
valc# = -1 * Kp#
sqrval# = (valb# ^ 2 – 4 * vala# * valc#)
molCO1# + (-1 * valb# + Sqr(sqrval#)) / (2 * vala#)
molCO2# = (-1 * valb# - Sqr(sqrval#)) / (2 * vala#)
If molCO1# > 0 Then
    If molCO1# < 1 Then
        TruemolCO# = molCO1#
        GoTo defined:
    Else
        TruemolCO# = molCO2#
    End If
Else
    TruemolCO# = molCO2#
End If
defined:
ansCO2# = ((1 – TruemolCO#) / 2)
ansCO# = (TruemolCO# / 2)
TB_CO.Text = Str(ansCO#)
TB_CO2.Text = Str(ansCO2#)
Kp2# = Exp((33965.169 / Truetemp#) – 10.441)
PPO2# = Log((ansCO2# / (ansCO# * Kp2#)) ^ 2) / Log(10)
TB_PPO2.Text = Str(PPO2#)
finito:
End Sub
```

REFERENCES

1) Borchardt, H.J., and Bierstedt, P.E., "$Gd_2(MoO_4)_3$: A Ferroelectric Laser Host," *Applied Physics Letters*, 8 [2] 50-52 (1966).

2) Leichtfried, G., and Wetzel, S., *12th International Plansee Seminar*, 1, 1023, 1989

3) Endo, M., Kimur, K., Udagawa, T., Tanabe, S., and Seto, H., "The Effects of doping Molybdenum Wire with Rare-Earth Elements," *High Temperatures-High Pressures*, 22 [2] 129-137 (1990).

4) Leichtfried, G., "Molybdenum Lanthanum Oxide: Special material properties by dispersoid refining during deformation," *Advances in Powder Metallurgy & Particulate Materials – vol. 9*, Proceedings of the 1992 Powder Metallurgy World Congress, San Francisco, CA (1992).

5) Zhang, J., Liu, L., Zhou, M., Hu, Y., and Zuo, T., "Fracture Toughness of Sintered Mo-La_2O_3 alloy and the Toughening," *International Journal of Refractory Metals & Hard Materials*, 17 [6] 405-409 (1999).

6) Fournier, J., Fournier, J., and Kohlmuller, R., "Etude des systemes La_2O_3-MoO_3, Y_2O_3-MoO_3, et des phases Ln_6MoO_{12}," *Bulletin de la Societe Chimique de France*, [12] 4277-83 (1970).

7) Brixner, L.H., Sleight, A.W., and Licis, M.S., "Cell Dimensions of the Molybdates $La_2(MoO_4)_3$, $Ce_2(MoO_4)_3$, $Pr_2(MoO_4)_3$, and $Nd_2(MoO_4)_3$," *Journal of Solid State Chemistry*, 5, 247-249 (1972).

8) Brixner, L.H., Sleight, A.W., and Licis, M.S., "Ln_2MoO_6-Type Rare Earth Molybdates – Preparation and Lattice Parameters," *Journal of Solid State Chemistry*, 5, 186-190 (1972).

9) Hubert, P., "Monomolybdites des terres rares Ln_2MoO_5 (Ln-La a Lu + Y)," *C. R. Acad. Sc. Paris*, 285 (1977).

10) Kerner-Czeskleba, H., and Tourne, G., "Preparation de Nouveaux Oxydes de Molybdene IV et de Lanthanide de Formule Ln_2MoO_5," *Materials Research Bulletin*, 13, 271-278 (1978).

11) Kerner-Czeskleba, H., and Cros, B., "Synthesis and Characterization of Flourite Related Molybdates $Ln_{12}Mo_6O_{35}$." *Materials Research Bulletin*, 13, 947-952 (1978).

12) Nassau, K., and Shiever, J.W., "Structural and phase relationships among trivalent tungstates and molybdates," *NBS Solid State Chem* 445-456 (1972).

13) Megumi, K., Yumoto, H., Ashida, S., Akiyama, S., and Furuhata, Y. "Phase Equilibrium Diagram for the System Gd_2O_3-MoO_3," *Materials Research Bulletin*, 9, 391-400 (1974).

14) Kerner-Czeskleba, H., "Phase Equilibrium and Compound Formation in Rare Earth-Molybdenum-Oxide Systems, Ln_2O_3-MoO_2-MoO_3," Third International Conference on the Chemistry and Uses of Molybdenum, Ann Arbor, MI (1979).

15) Czeskleba-Kerner, H., Cros, B., and Tourne, G., "Phase Equilibria and Compound Formation in the Nd-Mo-O system between 1273 and 1673K," *Journal of Solid State Chemistry*, 37, 294-301 (1981).

16) Prevost-Czeskleba, H., and Tourne, G., "Phase Studies and Selective Oxidation in Rare Earth-Molybdenum-Oxide systems, Ln_2O_3-MoO_2-MoO_3," *Rare Earths Mod. Sci. Technol.*, 3, 271-274 (1982).

17) McCarroll, W.H., Darling, C., and Jakubicki, G., "Synthesis of Reduced Comples Oxides of Molybdenum by Fused Salt Electrolysis," *Journal of Solid State Chemistry*, 48, 189-195 (1983).

18) Moini, A., Subramanian, M.A., Clearfield, A., DiSalvo, F.J., and McCarroll, W.H., "Structure and Properties of $La_2Mo_2O_7$: a Quasi-Two-Dimensional Metallic Oxide with Strong Mo-Mo Bonds," *Journal of Solid State Chemistry*, 66, 136-143 (1987).

19) Huang, Q., Xu, J., and Li, W., "Preparation of Tetragonal Defect Scheelite Type $RE_2(MoO_4)_3$ (RE=La to Ho) by Precipitation Method," *Solid State Ionics*, 32/33, 244-249 (1989).

20) Fournier, J.P., Fournier, J., and Kohlmuller, R., *Bull. Soc. Chim. France*, [12] 4278 (1970).

21) Alekseev, *et al.*, *Russ. J. Inorg. Chem.*, 14, 1558 (1969).

22) McIlvried, and McCarthy, Penn State University, University Park, PA (1972).

23) Cros, B., and Kerner-Czeskleba, H., "Synthesis and Characterization of Stable Compounds at 1400 degrees C from the system La_2O_3-MoO_2-MoO_3," *Revue de Chimie Minerale*, 15 [6] 521-528 (1978).

24) Shi, F., Meng, J., and Ren, Y., *Solid State Commun*., 95, 745 (1995).

25) Hubert, P., *Compt. Rend. Seances Acad. Sci., Ser. C*, 259, 2238 (1964).

26) Hubert, P.H., *Compt. Rend. Seances Acad. Sci.*, 260, 3677, (1965).

27) Hubert, P.H., Michel, P., and Vincent, C., *Compt. Rend. Hebd. Seances Acad. Sci., Ser. C* 269, 1287-1289 (1969).

28) Hubert, P., *Bulletin Societe Chimique de France*, 475 (1975).

29) Gall, P., and Gougeon, P. "Structure of $La_4Mo_2O_{11}$ Containing Isolated Mo_2O_{10} Cluster Units," *Acta Crystallography*, C48, 1915-1917 (1992).

30) Reimers, J.N., Greedan, J.E., and Sato, M., "The Crystal Structure of Spin Glass Pyrochlore, $Y_2Mo_2O_7$," *Journal of Solid State Chemistry*, 72, 390-394 (1988).

31) Torardi, C., Fecketter, C., McCaroll, W.H., and Disalvo, F.J., "Structure and Properties of $Y_5Mo_2O_{12}$ and $Gd_5Mo_2O_{12}$: Mixed Valence Oxides with structurally Equivalent Molybdenum Atoms," *Journal of Solid State Chemistry*, 60, 332-343 (1985).

32) Stedman, N.J., Cheetham, A.K., and Battle, P.D., "$YMoO_4$ Revisited: The Crystal Structure of YMo_4O_{18}," *J. Mater. Chem.*, 4 [9] 1457-1461 (1994).

33) Trunov, V.K., and Kovba, L.M., *Russian Journal of Inorganic Chemistry*, 12, 1703 (1967).

34) Tarte, P., and Auray, M., "Polymorphism of Zirconium Molybdate $Zr(MoO_4)_2$," Solid State Chemistry 1982, Proceedings of the Second European Conference, Veldhoven Netherlands (1982).

35) Auray, M., Quarton, M., and Tarte, P., "New Structure of High-Temperature Zirconium Molybdate," *Acta Crystallography*, C42, 257-259 (1986).

36) Hoch, M., and Desjardins, M., "The System Molybdenum-Titanium-Zirconium-Oxygen at 1500ºC," *Transactions of the Metallurgical Society of AIME*, 224, 821 (1962).

37) Ustinov, O.A., Novoselov, G.P., Andrianov, M.A., and Chevotarev, N.T., *Russian Journal of Inorganic Chemistry*, 15, 1318 (1970).

38) Bart, J.C.J., and Giordano, N., "Phase Relationships in the Cerium-Molybdenum Oxide System," *Journal of the Less-Common Metals*, 46, 17-24 (1976).

39) Hill, G., M.S. Thesis, *Georgia Institute of Technology* (2003).